Polarization Gradients in A Two Chambered Cell

Jaideep Singh
University of Virginia

Aidan M. Kelleher
The College of William and Mary

Patricia H. Solvignon
Medium Energy Physics Group, Argonne National Laboratory

Version 1.37

December 6, 2006

Abstract

We show that the relative difference in polarization between the pumping and target chambers depends on the ratio of the target chamber spin-relaxation rate to the target chamber diffusion rate. A collection of parameters and formulas necessary for the calculation of these two rates are presented.
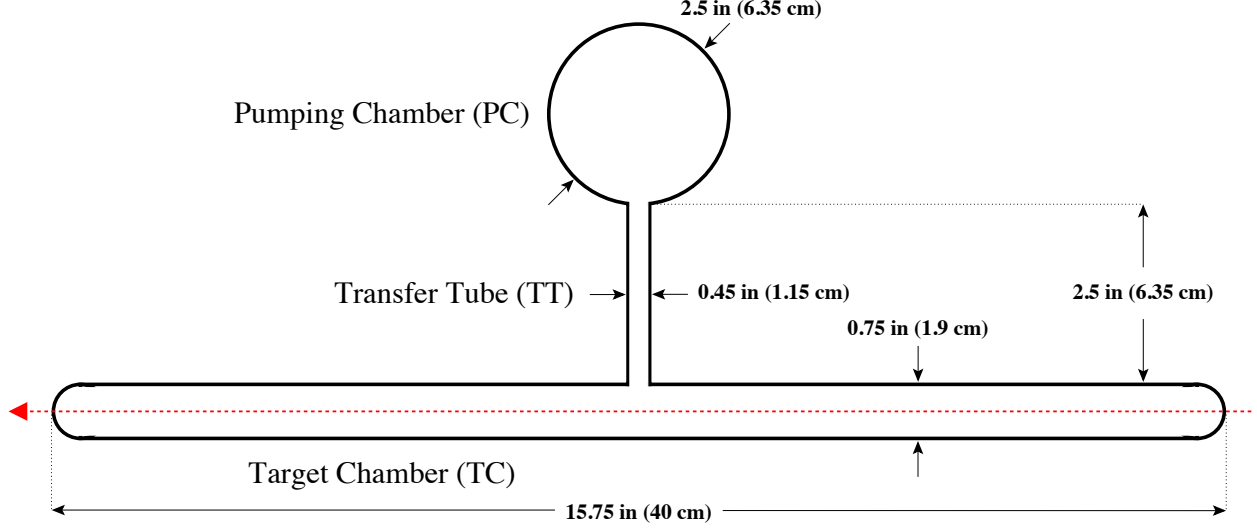
Contents

Figure 1: Basic Geometry of a "Standard" Small Pumping Chamber Cell. Drawn to scale with nominal outer dimensions. Dashed red line represents path of electron beam.

Element	k_{se} $\left(10^{-20}\ \mathrm{cm}^3/\mathrm{sec}\right)$	k_{se} $\left(1/\mathrm{hrs\ per\ }10^{14}\ \mathrm{cm}^{-3}\right)$	ref.
Rb	6.79 ± 0.20	$1/\left(40.9 \pm 1.2\right)$	[1]
K	6.1 ± 0.4	$1/\left(45.5 \pm 3.0\right)$	[2]
Na	6.1 ± 0.6	$1/\left(45.5 \pm 4.5\right)$	[3]

Table 1: Alkali-^{3}He Spin-Exchange Rate Constants.

1 Polarization Dynamics

1.1 Nuclei Number Rate Equations

A cell is composed of a pumping and target chamber that are connected by a transfer tube, see Fig. (1). In Sec. 3.2, we will consider in more detail the polarization dynamics within the transfer tube; however, for now, we will simply ignore the small transfer tube volume. The ^{3}He nuclei in the pumping chamber are polarized via spin-exchange collisions with polarized alkali atoms with a rate constant k_{se}, see Tab. (1). The ^{3}He nuclei in the target chamber are polarized via diffusion through the transfer tube. Because of the low alkali vapor pressure in the target chamber, we will ignore the spin exchange with alkali atoms in the target chamber. The number of ^{3}He nuclei is $N_{pc,tc}^{\pm}$ where the superscript $\pm$ labels the spin state and the subscript labels the chamber. Similarly the total number of ^{3}He nuclei in a given chamber is $N_{pc,tc}\left(= N_{pc,tc}^{+} + N_{pc,tc}^{-}\right)$. Consequently the total number of ^{3}He nuclei is $N\left(= N_{pc} + N_{tc}\right)$ and the fraction of ^{3}He nuclei in either chamber is $f_{pc,tc}\left(= N_{pc,tc}/N\right)$.

Assuming that the alkali polarization reaches equilibrium very quickly and remains constant while the ^{3}He polarization approaches equilbrium, the rate of change of the number of $\pm$ nuclei in either chamber is governed by the following equations:

$$\frac{dN_{pc}^{+}}{dt} = k_{se}[A^{+}]N_{pc}^{-} - k_{se}[A^{-}]N_{pc}^{+} + \left(\frac{N_{pc}}{2} - N_{pc}^{+}\right)\Gamma_{pc} + N_{tc}^{+}d_{tc} - N_{pc}^{+}d_{pc}$$

$$\frac{dN_{pc}^{-}}{dt} = k_{se}[A^{-}]N_{pc}^{+} - k_{se}[A^{+}]N_{pc}^{-} + \left(\frac{N_{pc}}{2} - N_{pc}^{-}\right)\Gamma_{pc} + N_{tc}^{-}d_{tc} - N_{pc}^{-}d_{pc}$$

$$\frac{dN_{tc}^{+}}{dt} = N_{pc}^{+}d_{pc} - N_{tc}^{+}d_{tc} + \left(\frac{N_{tc}}{2} - N_{tc}^{+}\right)\Gamma_{tc}$$

$$\frac{dN_{\text{tc}}^-}{dt} \;=\; N_{\text{pc}}^- d_{\text{pc}} - N_{\text{tc}}^- d_{\text{tc}} + \left(\frac{N_{\text{tc}}}{2} - N_{\text{tc}}^-\right)\Gamma_{\text{tc}} \tag{1}$$

where $[A^{\pm}]$ is the alkali number density in the pumping chamber for the $\pm$ spin state. The spin-relaxation rates per nucleus $\Gamma_{\text{pc,tc}}$ represent interactions which show no preference for either state and therefore push equilibrium towards equal numbers of $\pm$ nuclei. The diffusion rate $d_{\text{tc(pc)}}$ is the probability per unit time per nucleus that a nucleus will exit the target (pumping) chamber and enter the pumping (target) chamber, where we have neglected the transfer tube volume. The rates of change of the total number of nuclei in the two chambers are given by:

$$\frac{dN_{\text{pc}}}{dt} \;=\; \frac{dN_{\text{pc}}^+}{dt} + \frac{dN_{\text{pc}}^-}{dt} = N_{\text{tc}} d_{\text{tc}} - N_{\text{pc}} d_{\text{pc}}$$

$$\frac{dN_{\text{tc}}}{dt} \;=\; \frac{dN_{\text{tc}}^+}{dt} + \frac{dN_{\text{tc}}^-}{dt} = N_{\text{pc}} d_{\text{pc}} - N_{\text{tc}} d_{\text{tc}}$$

$$\frac{dN}{dt} \;=\; \frac{dN_{\text{pc}}}{dt} + \frac{dN_{\text{tc}}}{dt} = 0 \tag{2}$$

When the total number of nuclei in either chamber reaches equilibrium, the total diffusion rates into and out of each chamber must balance:

$$N_{\text{tc}} d_{\text{tc}} = N_{\text{pc}} d_{\text{pc}} \qquad \rightarrow \qquad f_{\text{tc}} d_{\text{tc}} = f_{\text{pc}} d_{\text{pc}} \tag{3}$$

1.2 Polarization Rate Equations

Polarization for any spin-1/2 particle is defined as:

$$P_{\text{pc,tc}} \;=\; \frac{N_{\text{pc,tc}}^+ - N_{\text{pc,tc}}^-}{N_{\text{pc,tc}}^+ + N_{\text{pc,tc}}^-} = \frac{N_{\text{pc,tc}}^+ - N_{\text{pc,tc}}^-}{N_{\text{pc,tc}}} = f_{\text{pc,tc}}^+ - f_{\text{pc,tc}}^- \tag{4}$$

Combining the nuclei number rate Eqns. (1) in the manner defined above, noting the following relationships:

$$f_{\text{pc,tc}}^{\pm} = \frac{1}{2}\left(1 \pm P_{\text{pc,tc}}\right) \qquad\qquad f_{\text{pc,tc}} = f_{\text{pc,tc}}^+ + f_{\text{pc,tc}}^- \qquad\qquad 1 = f_{\text{pc}} + f_{\text{tc}} \tag{5}$$

and, to reiterate, assuming that the alkali polarization reaches equilibrium very quickly and remains constant during the ^{3}He polarization build-up, the polarizations in the two chambers of the cell are given by:

$$\frac{dP_{\text{pc}}}{dt} \;=\; \gamma_{\text{se}}\left(P_A - P_{\text{pc}}\right) - \Gamma_{\text{pc}} P_{\text{pc}} - d_{\text{pc}} P_{\text{pc}} + \left(\frac{d_{\text{tc}} N_{\text{tc}}}{N_{\text{pc}}}\right) P_{\text{tc}}$$

$$\frac{dP_{\text{tc}}}{dt} \;=\; \left(\frac{d_{\text{pc}} N_{\text{pc}}}{N_{\text{tc}}}\right) P_{\text{pc}} - d_{\text{tc}} P_{\text{tc}} - \Gamma_{\text{tc}} P_{\text{tc}} \tag{6}$$

where γ_{se} $(= k_{\text{se}}[A])$ is the spin-exchange rate per nucleus and P_A is the pumping chamber volume averaged equilibrium alkali polarization. If we assume that the total nuclei number in each chamber has reached equilibrium before the polarization process is initiated (i.e. the cell is brought to operating temperature before the lasers are turned on), then we can take advantage of the relationship defined by Eqn. (3) to give the following:

$$\frac{dP_{\text{pc}}}{dt} \;=\; \gamma_{\text{se}}\left(P_A - P_{\text{pc}}\right) - \Gamma_{\text{pc}} P_{\text{pc}} - d_{\text{pc}}\left(P_{\text{pc}} - P_{\text{tc}}\right) = a P_{\text{pc}} + b P_{\text{tc}} + B \tag{7}$$

$$\frac{dP_{\text{tc}}}{dt} \;=\; d_{\text{tc}}\left(P_{\text{pc}} - P_{\text{tc}}\right) - \Gamma_{\text{tc}} P_{\text{tc}} = c P_{\text{pc}} + d P_{\text{tc}} \tag{8}$$

where the following substitutions are made:

$$a = -\left(\gamma_{\text{se}} + \Gamma_{\text{pc}} + d_{\text{pc}}\right) \qquad b = d_{\text{pc}} \qquad c = d_{\text{tc}} \qquad d = -\left(\Gamma_{\text{tc}} + d_{\text{tc}}\right) \qquad B = \gamma_{\text{se}} P_A \tag{9}$$

The coupled rate equations can be rewritten as a matrix equation:

$$\frac{d}{dt}\begin{bmatrix} P_{\text{pc}} \\ P_{\text{tc}} \end{bmatrix} = \begin{bmatrix} a & b \\ c & d \end{bmatrix}\begin{bmatrix} P_{\text{pc}} \\ P_{\text{tc}} \end{bmatrix} + \begin{bmatrix} B \\ 0 \end{bmatrix} \qquad \rightarrow \qquad \frac{d\vec{P}}{dt} = \mathbf{M}\vec{P} + \vec{B} \tag{10}$$

1.3 Analytic Solution to Polarization Rate Equations

Eqn. (10) is solved by finding the eigenvalues of the rate matrix $\mathbf{M}$. These eigenvalues:

$$\Gamma_\pm = -\frac{1}{2}\left[a + d \pm \sqrt{(a-d)^2 + 4bc}\right] \tag{11}$$

are the characteristic rates of the system and, as will be explained shortly, are labeled slow and fast:

$$\Gamma_{\rm s} = \frac{1}{2}\left[d_{\rm pc}+d_{\rm tc}+\gamma_{\rm se}+\Gamma_{\rm pc}+\Gamma_{\rm tc}-\sqrt{(d_{\rm pc}+d_{\rm tc})^2+2\left(d_{\rm pc}-d_{\rm tc}\right)\left(\gamma_{\rm se}+\Gamma_{\rm pc}-\Gamma_{\rm tc}\right)+\left(\gamma_{\rm se}+\Gamma_{\rm pc}-\Gamma_{\rm tc}\right)^2}\right] \tag{12}$$

$$\Gamma_{\rm f} = \frac{1}{2}\left[d_{\rm pc}+d_{\rm tc}+\gamma_{\rm se}+\Gamma_{\rm pc}+\Gamma_{\rm tc}+\sqrt{(d_{\rm pc}+d_{\rm tc})^2+2\left(d_{\rm pc}-d_{\rm tc}\right)\left(\gamma_{\rm se}+\Gamma_{\rm pc}-\Gamma_{\rm tc}\right)+\left(\gamma_{\rm se}+\Gamma_{\rm pc}-\Gamma_{\rm tc}\right)^2}\right] \tag{13}$$

The solutions to the coupled rate equations are given by:

$$P_{\rm pc}(t) = P_{\rm pc}^\infty + \left[P_{\rm pc}^0 - P_{\rm pc}^\infty - c_{\rm pc}\right]\exp\left(-\Gamma_{\rm s}t\right) + c_{\rm pc}\exp\left(-\Gamma_{\rm f}t\right) \tag{14}$$

$$P_{\rm tc}(t) = P_{\rm tc}^\infty + \left[P_{\rm tc}^0 - P_{\rm tc}^\infty - c_{\rm tc}\right]\exp\left(-\Gamma_{\rm s}t\right) + c_{\rm tc}\exp\left(-\Gamma_{\rm f}t\right) \tag{15}$$

where $P_{\rm pc,tc}^0$ are set by the initial conditions and the equilibrium ($t \to \infty$) polarizations are found by setting the rate equations to zero:

$$P_{\rm pc}^\infty = \frac{B}{bc - ad} \qquad \& \qquad P_{\rm tc}^\infty = -\left(\frac{c}{d}\right)P_{\rm pc}^\infty \tag{16}$$

The above can be written in a more illuminating form by using Eqn. (3) and after some algebra:

$$P_{\rm pc}^\infty = P_A\left[\frac{\gamma_{\rm se}f_{\rm pc}}{\gamma_{\rm se}f_{\rm pc} + \Gamma_{\rm pc}f_{\rm pc} + \Gamma_{\rm tc}f_{\rm tc}\left(1 + \frac{\Gamma_{\rm tc}}{d_{\rm tc}}\right)^{-1}}\right] \tag{17}$$

$$P_{\rm tc}^\infty = P_{\rm pc}^\infty\left[1 + \frac{\Gamma_{\rm tc}}{d_{\rm tc}}\right]^{-1} \tag{18}$$

Finally, the coefficients $c_{\rm pc,tc}$ can be obtained by satisfying the coupled rate equations and after some algebra:

$$c_{\rm pc} = \frac{\Gamma_{\rm s}\left(P_{\rm pc}^\infty - P_{\rm pc}^0\right) - bP_{\rm tc}^0 - aP_{\rm pc}^0 - B}{\Gamma_{\rm f} - \Gamma_{\rm s}} \tag{19}$$

$$c_{\rm tc} = \frac{\Gamma_{\rm s}\left(P_{\rm tc}^\infty - P_{\rm tc}^0\right) - dP_{\rm tc}^0 - cP_{\rm pc}^0}{\Gamma_{\rm f} - \Gamma_{\rm s}} \tag{20}$$

1.4 Fast Diffusion Limit

In the limit where the diffusion rates are very fast compared to all other rates, the response of the system to lowest order is characterized by:

$$\Gamma_{\rm s} = \langle\gamma_{\rm se}\rangle + \langle\Gamma\rangle - \delta\Gamma \tag{21}$$

$$\Gamma_{\rm f} = (d_{\rm pc} + d_{\rm tc}) + (\gamma_{\rm se} - \langle\gamma_{\rm se}\rangle) + (\Gamma_{\rm pc} + \Gamma_{\rm tc} - \langle\Gamma\rangle) + \delta\Gamma \tag{22}$$

where again we have made use of Eqn. (3) in the form of:

$$\frac{d_{\rm pc} - d_{\rm tc}}{d_{\rm pc} + d_{\rm tc}} = \frac{d_{\rm tc}\left(\frac{f_{\rm tc}}{f_{\rm pc}}\right) - d_{\rm tc}}{d_{\rm tc}\left(\frac{f_{\rm tc}}{f_{\rm pc}}\right) + d_{\rm tc}} = \frac{f_{\rm tc} - f_{\rm pc}}{f_{\rm tc} + f_{\rm pc}} = f_{\rm tc} - f_{\rm pc} \tag{23}$$

and we have defined the following quantities to lowest order:

$$\langle \gamma_{\rm se} \rangle \equiv \gamma_{\rm se} f_{\rm pc} \tag{24}$$

$$\langle \Gamma \rangle \equiv \Gamma_{\rm pc} f_{\rm pc} + \Gamma_{\rm tc} f_{\rm tc} \tag{25}$$

$$\delta\Gamma \equiv f_{\rm pc} f_{\rm tc} \frac{(\gamma_{\rm se} + \Gamma_{\rm pc} - \Gamma_{\rm tc})^2}{d_{\rm pc} + d_{\rm tc}} + \mathcal{O}\left(\frac{(\gamma_{\rm se} + \Gamma_{\rm pc} - \Gamma_{\rm tc})^3}{(d_{\rm pc} + d_{\rm tc})^2}\right) \tag{26}$$

where the brackets $\langle \cdots \rangle$ refer to an average over all nuclei. Fig. (2) depicts the slow and fast time constants (note that a time constant is defined to be the inverse rate, $\tau \equiv 1/\gamma$) to different orders for two cell types.

In the limit $d_{\rm pc,tc} \to \infty$, the equilibrium polarizations and coefficients become:

$$P_{\rm pc}^\infty \to P_A \left[\frac{\gamma_{\rm se} f_{\rm pc}}{\gamma_{\rm se} f_{\rm pc} + \Gamma_{\rm pc} f_{\rm pc} + \Gamma_{\rm tc} f_{\rm tc}}\right] = P_A \left[\frac{\langle \gamma_{\rm se} \rangle}{\langle \gamma_{\rm se} \rangle + \langle \Gamma \rangle}\right] \tag{27}$$

$$P_{\rm tc}^\infty \to P_{\rm pc}^\infty \tag{28}$$

$$c_{\rm pc} \to f_{\rm pc} \left(P_{\rm tc}^0 - P_{\rm pc}^0\right) \tag{29}$$

$$c_{\rm tc} \to f_{\rm tc} \left(P_{\rm pc}^0 - P_{\rm tc}^0\right) \tag{30}$$

which gives for the polarizations in the two chambers:

$$P_{\rm pc}(t) = P_{\rm pc}^\infty + \left[P_{\rm pc}^0 f_{\rm pc} + P_{\rm tc}^0 f_{\rm tc} - P_{\rm pc}^\infty\right] \exp\left(-\Gamma_{\rm s} t\right) + f_{\rm pc} \left[P_{\rm tc}^0 - P_{\rm pc}^0\right] \exp\left(-\Gamma_{\rm f} t\right) \tag{31}$$

$$P_{\rm tc}(t) = P_{\rm pc}^\infty + \left[P_{\rm pc}^0 f_{\rm pc} + P_{\rm tc}^0 f_{\rm tc} - P_{\rm pc}^\infty\right] \exp\left(-\Gamma_{\rm s} t\right) + f_{\rm tc} \left[P_{\rm pc}^0 - P_{\rm tc}^0\right] \exp\left(-\Gamma_{\rm f} t\right) \tag{32}$$

After the fast exponential has decayed away, the polarization in the two chambers evolves identitically as if the initial polarization in the two chambers had been a volume of average of the true initial polarizations in the two chambers:

$$P(t) = P_{\rm pc}(t) = P_{\rm tc}(t) = P_{\rm pc}^\infty \left[1 - \exp\left(-\Gamma_{\rm s} t\right)\right] + \left[P_{\rm pc}^0 f_{\rm pc} + P_{\rm tc}^0 f_{\rm tc}\right] \exp\left(-\Gamma_{\rm s} t\right)$$

$$= P^\infty \left[1 - \exp\left(-\Gamma_{\rm s} t\right)\right] + \langle P^0 \rangle \exp\left(-\Gamma_{\rm s} t\right) \tag{33}$$

2 Relaxation Mechanisms

2.1 Spin Relaxation Due to Nuclear Dipolar Interactions

The theoretical minimum spin-relaxation rate is due to a direct coupling between two nearby ^{3}He nuclei. Newbury et al. [4] have calculated this ^{3}He-^{3}He nuclear dipolar spin-relaxation rate per nucleus at 23 °C:

$$\Gamma_{\rm dip} = \frac{\left[^3{\rm He}\right]}{(744~{\rm amg} \cdot {\rm hrs})} \tag{34}$$

Fig. (3) [4, adapted from Figs. 2 and 3] depicts the temperature dependence of the relaxation rate from 0 K to 10 K and 1 K to 550 K calculated using one particular choice for the He-He interatomic potential. Newbury et al. state that two alternative models for the interatomic potential give consistent results within a few percent. An analytical form of the temperature dependence is not given; therefore we have prepared a "homemade" parameterization of this curve:

$$\Gamma_{\rm dip} = \frac{\left[^3{\rm He}\right]}{(744~{\rm amg} \cdot {\rm hrs}) \cdot f_{\rm dip}(T)} \tag{35}$$

$$f_{\rm dip}(T) = c_0 \cdot \left(\frac{T}{T_0}\right)^{c_1} + c_2 + c_3 \cdot \left(\frac{T}{T_0}\right) + \frac{c_4}{1 + c_5 \cdot \frac{T}{T_0}} \tag{36}$$

where the values of the parameters are listed in Tab. 2. Note that at $T = T_0 = 23$ °C $= 296.15$ K, the

5
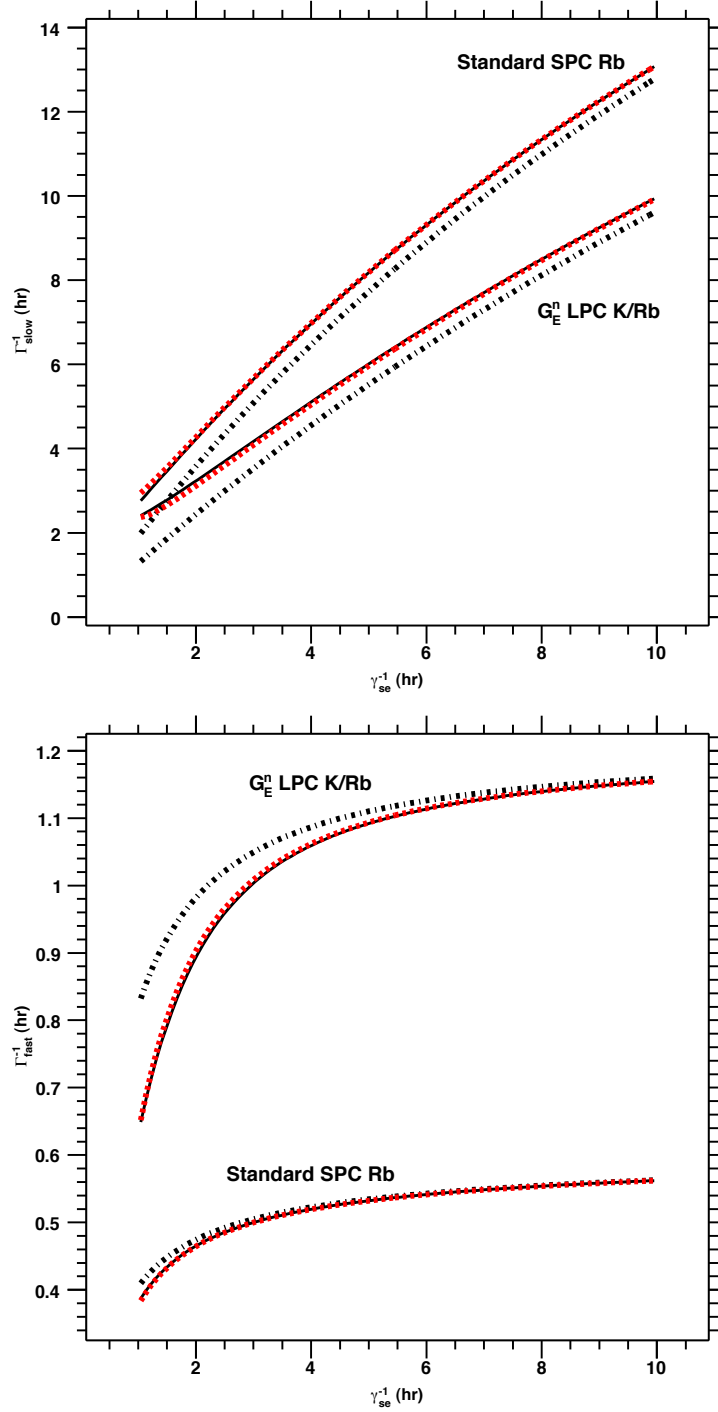
Figure 2: Slow (upper) and Fast (lower) Time Constants for Two Chambered Cells. Time constants (inverse rates) are plotted as a function of the spin-exchange time constant (γ_{se}^{-1}). Leading order (dotted black), next to leading order (dashed red), and full (solid black) calculations are depicted. The next to leading order (dashed red) is nearly identical to the full calculation (solid black). A typical "Standard SPC Rb" cell has dimensions $L_{tt} = 6$ cm & $V_{pc} = 90$ cc and contains pure Rb; whereas a typical "G_E^n LPC K/Rb" cell has dimensions $L_{tt} = 9$ cm & $V_{pc} = 310$ cc and contains a hybrid mix of mostly K and some Rb. The observed spin-up time constant, which is essentially Γ_s^{-1}, is always longer than the spin-exchange time constant. In addition, the spin-up time constants for the two different cells converge for sufficiently fast spin exchange.

Figure 3: Temperature Dependence of Nuclear Dipolar Relaxation for a Density of 10 Amagats. Note that both vertical axes are the spin-relaxation time constants Γ_{dip}^{-1}. Red points were located "by eye" from Figs. (2) & (3) in [4]. Black curve i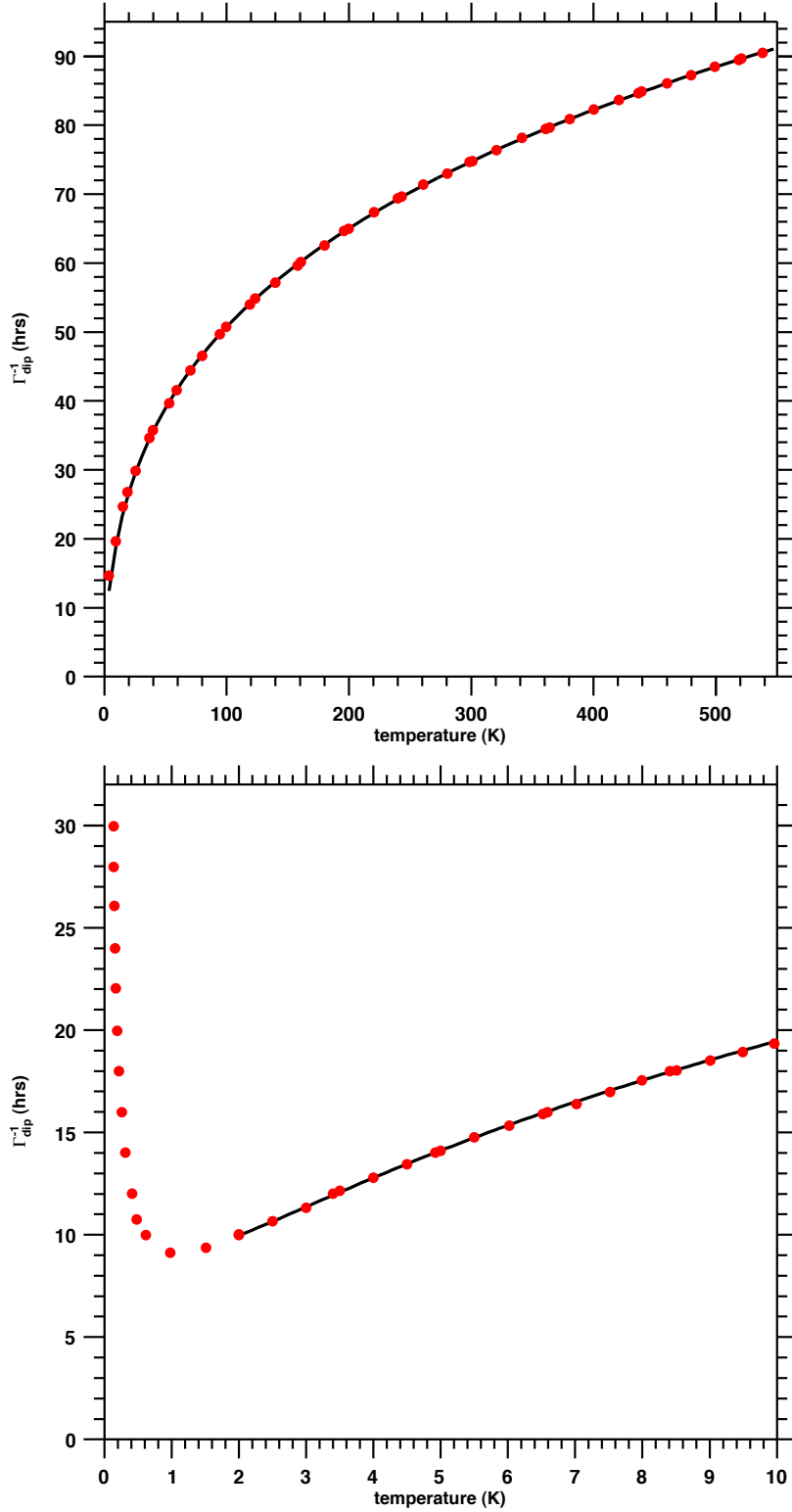s the parameterization, Eqn. (36), that was fit to the red points. They agree to better than half a percent from 2 K to 550 K.

parameter	value
c_0	+1.2319E+0
c_1	+2.8591E−1
c_2	−2.1793E−1
c_3	−1.4426E−2
c_4	+5.3315E−1
c_5	+1.2376E+3
T_0	296.15 K

Table 2: Parameters for Nuclear Dipolar Relaxation Temperature Dependence Eqn. (36). Except for T_0, all parameters are unitless.

temperature function f_{dip} equals 1 as expected:

$$f_{\text{dip}}(T_0) = c_0 + c_2 + c_3 + \frac{c_4}{1 + c_5} = 1 \tag{37}$$

This parameterization reproduces the curve in Fig. (3) to better than 0.5% from 2 K to 550 K. All things considered, a reasonable estimate for the uncertainty associated with this calculation/parameterization is about 5%.

2.2 Basic Mechanism of Beam Depolarization

Ionizing radiation increases the nuclear spin relaxation in the target chamber. Also known as "beam depolarization," it is essentially a two step process. First, the beam ionizes an ^{3}He atom which results in an free electron and an atomic ion ^{3}He$^+$. There is also the possibility that the atomic ion bonds with an neutral ^{3}He atom to form an molecular ion ^{3}He$_2^+$. Second, interactions with ^{3}He ions induce ^{3}He nuclear spin flips. Therefore, the total relaxation rate due to ionization by the beam is given by:

$$\Gamma_{\text{beam}} = \left[\begin{array}{c} \text{ionization rate} \\ \text{per target chamber atom} \end{array} \right] \cdot \left[\begin{array}{c} \text{mean number of nuclear spin flips} \\ \text{per atomic ion} \end{array} \right] \tag{38}$$

$$= \left[\left(\begin{array}{c} \text{electrons} \\ \text{per unit time} \end{array} \right) \cdot \left(\begin{array}{c} \text{atomic ions created} \\ \text{per electron} \end{array} \right) \right] \cdot \left[(\text{atoms in tc})^{-1} \cdot (n_a + n_m) \right] \tag{39}$$

$$= \left[\left(\frac{I}{e} \right) \cdot \left(\frac{\text{total energy lost}}{\text{mean energy per ion}} \right) \right] \cdot \left[\left(\frac{1}{V_{\text{tc}} [\text{He}]_{\text{tc}}} \right) \cdot (n_a + n_m) \right] \tag{40}$$

$$= \left[\left(\frac{I}{e} \right) \cdot \left(\frac{\left[\frac{1}{\rho} \frac{dE}{dx} \right] L_{\text{tc}} [\text{He}]_{\text{tc}}}{E_i} \right) \right] \cdot \left[\left(\frac{1}{V_{\text{tc}} [\text{He}]_{\text{tc}}} \right) \cdot (n_a + n_m) \right] \tag{41}$$

$$= \left(\frac{I}{e} \right) \cdot \left(\frac{1}{E_i} \left[\frac{1}{\rho} \frac{dE}{dx} \right] \frac{1}{A_{\text{tc}}} \right) \cdot (n_a + n_m) \tag{42}$$

$$= \Gamma_{\text{ion}} \cdot (n_a + n_m) \tag{43}$$

where I is the electron beam current, E_i is the mean energy for ion-electron pair creation, A_{tc} is the mean cross sectional area of the target chamber, Γ_{ion} is the ionization rate per ^{3}He atom in the target chamber, and n_a & n_m are the average number of spins lost per atomic ion created due to interactions with atomic & molecular ions respectively.

2.3 Beam Energy Lost to Ionizing Interactions

The electron beam loses energy to collisions and to radiation in the form of bremsstrahlung. At JLab energies, the dominant mode of *energy loss* is bremsstrahlung, see Fig (4). We will show, however, that the dominant
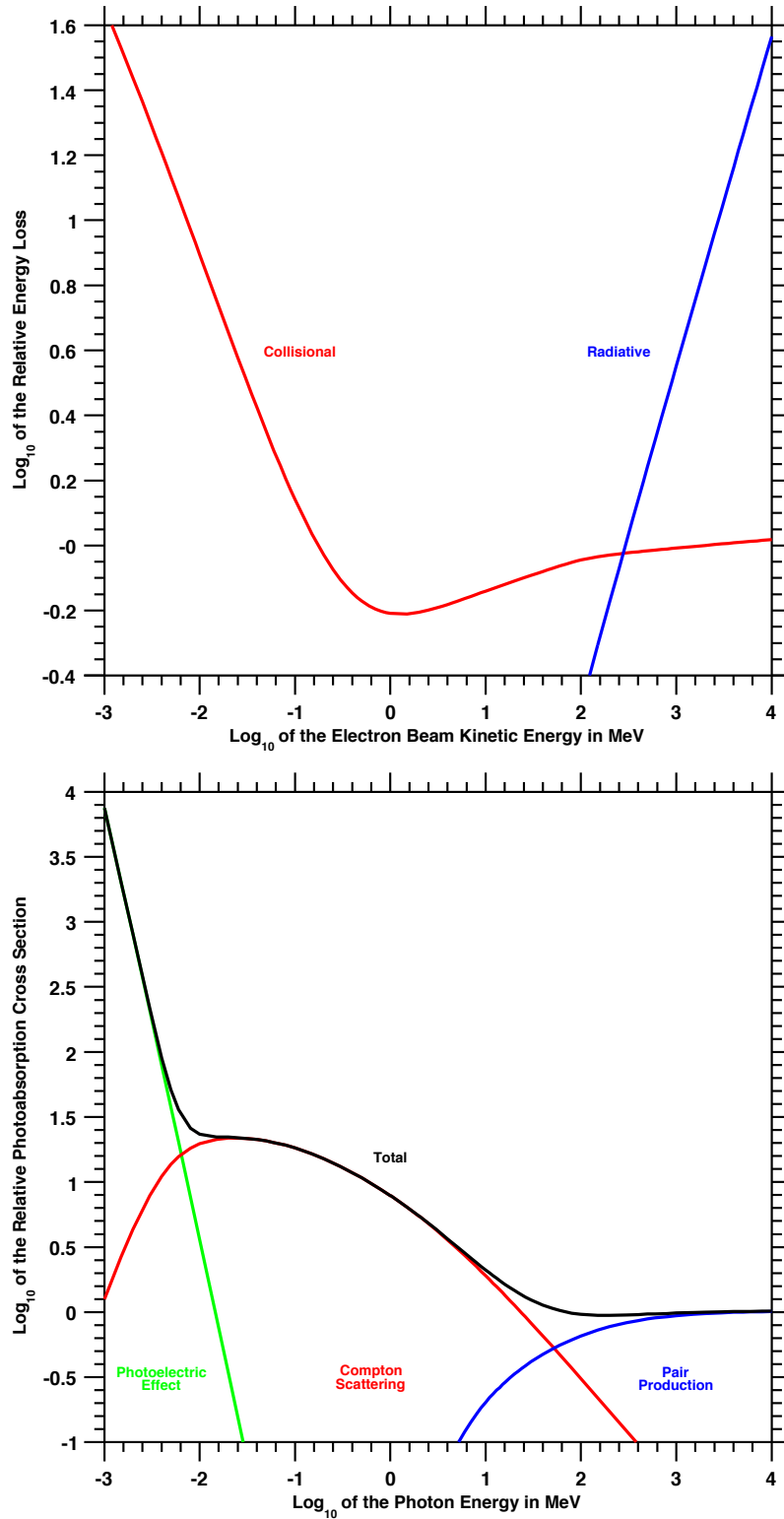
Figure 4: Upper: Relative Energy Loss to Collisions and to Radiation for Electrons in Helium. Energy loss is relative to the collisional energy loss for an electron beam energy of 2 GeV. Data is from NIST-ESTAR [5]. Lower: Relative Photoabsorption Cross Sections in Helium. Cross section is relative to the total photoabsorption cross section of a 2 GeV photon. Data is from NIST-XCOM [6].

parameter	value	comments
Z	2	atomic number
I_{BB}	41.8 eV	mean excitation potential
C_δ	-11.1393	
X_0	2.2017	
X_1	3.6122	for density correction
a	0.13443	
m	5.8347	

Table 3: Bethe-Bloch Formula Parameters for Electron-Helium Interactions. All values taken from [8].

mode of *ionization* is collisional energy loss. The energy lost to collisions per unit density per unit length is given by the celebrated Bethe-Bloch formula and, for an electron beam, it is [7]:

$$\left[\frac{1}{\rho}\frac{dE}{dx}\right]_{\mathrm{c}} = 2\pi r_{\mathrm{e}}^2 m_{\mathrm{e}}c^2 \frac{Z}{\beta^2}\left[\log\left([\gamma-1]^2[\gamma+1]\right) + 2\log\left(\frac{m_{\mathrm{e}}c^2}{I_{\mathrm{BB}}}\right) - F(\gamma) - \delta - 2\frac{C_s}{Z}\right] \quad (44)$$

$$2\pi r_{\mathrm{e}}^2 m_{\mathrm{e}}c^2 = 6.85 \text{ eV/amagat/cm} \quad (45)$$

$$F(\gamma) = \left[1 + \frac{2}{\gamma} - \frac{1}{\gamma^2}\right]\log(2) - \frac{1}{8}\left[1 - \frac{1}{\gamma}\right]^2 - \frac{1}{\gamma^2} \quad (46)$$

$$\gamma = \frac{1}{\sqrt{1-\beta^2}} = \frac{E_{\mathrm{beam}}}{m_{\mathrm{e}}c^2} \quad (47)$$

where Z is the target atomic number, $\beta(= v/c)$ is the electron velocity relative to the speed of light, I_{BB} is the mean excitation potential of the target material, δ is the density correction, and C_s is the shell correction. The shell correction is significant only when the incident electron velocity is roughly equal to or slower than the bound electron orbital velocity. For JLab beam energies, this is not the case; therefore the shell correction will be neglected ($C_s = 0$). The density correction δ is given by [7, 8]:

$$\delta(X) = \begin{cases} 0 & X < X_0 \\ 4.6052X + C_\delta + a(X_1 - X)^m & X_0 < X < X_1 \\ 4.6052X + C_\delta & X > X_1 \end{cases} \quad (48)$$

$$X = \log_{10}(\beta\gamma) \quad (49)$$

where C_δ, X_0, X_1, a, and m depend on the target material and for He are listed in Tab. (3).

Collisional energy loss leads directly to ionization of atoms in the target material. On the other hand, energy loss to radiation ionizes atoms only if the emitted bremsstrahlung photons subsequently interact with the target atoms. To provide an upper limit for the ionization contribution from radiation, we assume the following:

1. The photoelectric effect, compton scattering, and pair production can all result in ionization.

2. One rescattered/reabsorbed bremstrahlung photon ionizes at most one atom.

3. Every photon must travel half the length of the target chamber before exiting.

The energy loss to radiation that contributes to ionization per unit density per unit length is given by:

$$\left[\frac{1}{\rho}\frac{dE}{dx}\right]_{\mathrm{ri}} = \left(\frac{\text{total energy lost to radiation}}{\text{per unit density per unit length}}\right) \cdot (\text{fraction of energy that ionizes}) \quad (50)$$

Bremsstrahlung can produce any number of photons with any energy such that the total energy does not exceed the energy of the incident electron. The probability that any of these photons subsequently ionizes

depends on its energy; therefore, we must convolute the bremsstrahlung spectrum with the total photoabsorption cross section over all photon energies:

$$\left[\frac{1}{\rho}\frac{dE}{dx}\right]_{\mathrm{ri}} = E\int_0^1 u\left[\frac{1}{\rho}\frac{d^2\Phi(u)}{du\cdot dx}\right]\langle f(u)\rangle\,du \tag{51}$$

where $u(=h\nu/E)$ (unitless) is the photon energy as a fraction of the electron energy, $d^2\Phi(u)/du\cdot dx$ is the number of bremsstrahlung photons created per frequency bin per unit length, and $\langle f(u)\rangle$ is the average fraction of photons reabsorbed/rescattered:

$$\langle f(u)\rangle = 1 - \exp\left(-\sigma_\gamma(u)[\mathrm{He}]_{\mathrm{tc}}L_{\mathrm{tc}}/2\right) \tag{52}$$

Bethe and Heitler [9] have shown that the energy per frequency bin of the bremsstrahlung spectrum is roughly constant, see Fig. (5), and when the electron energy is so high that complete screening can be assumed, this constant is [7]:

$$\Phi_{\mathrm{rad}} \equiv \int_0^1 u\left[\frac{1}{\rho}\frac{d^2\Phi(u)}{du\cdot dx}\right]du = 4Z^2r_e^2\alpha\left[\log\left(183Z^{-1/3}\right) + \frac{1}{18} - g(Z)\right] \tag{53}$$

$$4r_e^2\alpha = 2.318\ \mathrm{millibarns} \tag{54}$$

where $g(Z=2) = 2.56\times10^{-4}$ for He. This reduces the convolution integral to an integral over $\langle f(u)\rangle$:

$$\left[\frac{1}{\rho}\frac{dE}{dx}\right]_{\mathrm{ri}} \approx E\Phi_{\mathrm{rad}}\int_0^1\langle f(u)\rangle\,du = \left[\frac{1}{\rho}\frac{dE}{dx}\right]_{\mathrm{rad}}\int_0^1\langle f(u)\rangle\,du \tag{55}$$

To approximate this integral, we first note that small photon energies have large photoabsorption cross sections (see Fig. (4)) but represent a small frequency range in the bremsstrahlung spectrum. Therefore we separate $\langle f(u)\rangle$ into three rectangular frequency bins and find:

$$\begin{aligned}\int_0^1\langle f(u)\rangle\,du &\approx \sum_n u_n\langle f(u)\rangle_n = \frac{\left(10^{-2}\ \mathrm{MeV}\right)\cdot(1.00)}{E_{\mathrm{beam}}}\\ &\quad + \frac{\left(10\ \mathrm{MeV}\ -10^{-2}\ \mathrm{MeV}\right)\cdot(0.01)}{E_{\mathrm{beam}}} + \frac{\left(E_{\mathrm{beam}} - 10\ \mathrm{MeV}\ -10^{-2}\ \mathrm{MeV}\right)\cdot\left(3\times10^{-4}\right)}{E_{\mathrm{beam}}}\\ &\approx \frac{0.01\ \mathrm{MeV}}{E_{\mathrm{beam}}} + \frac{0.1\ \mathrm{MeV}}{E_{\mathrm{beam}}} + 3\times10^{-4}\\ &\approx \frac{0.11\ \mathrm{MeV}}{E_{\mathrm{beam}}} + 3\times10^{-4}\end{aligned} \tag{56}$$

Using the above approximation for the integral in Eqn. (51) and dividing by the energy loss due to collisions gives the following estimate for the ratio:

$$\eta \equiv \frac{\left[\frac{1}{\rho}\frac{dE}{dx}\right]_{\mathrm{ri}}}{\left[\frac{1}{\rho}\frac{dE}{dx}\right]_{\mathrm{c}}} \approx \frac{0.01 + 0.027\cdot\left(\frac{E_{\mathrm{beam}}}{1\ \mathrm{GeV}}\right)}{\log\left(\frac{E_{\mathrm{beam}}}{1\ \mathrm{GeV}}\right) + 37} \leq 0.01\ (\text{for } E_{\mathrm{beam}} \leq 15\ \mathrm{GeV}) \tag{57}$$

Even though the energy loss to radiation is about 3 to 30 times larger than the energy loss due to collisions at JLab energies, it contributes very little to the ionization. Above electron beam energies of 200 MeV, the following gives the energy loss to collisions in helium to better than one percent compared to the full formula Eqn. (44):

$$\left[\frac{1}{\rho}\frac{dE}{dx}\right]_{\mathrm{c}(\mathrm{e}^-/\mathrm{He})} = 4\pi r_e^2 m_e c^2\left[\log\left(\frac{E_{\mathrm{beam}}}{1\ \mathrm{GeV}}\right) + 37.0\right] \tag{58}$$

$$4\pi r_e^2 m_e c^2 = 510\ \mathrm{keV}\cdot\mathrm{barn} = 13.70\ \mathrm{eV/amagat/cm} \tag{59}$$
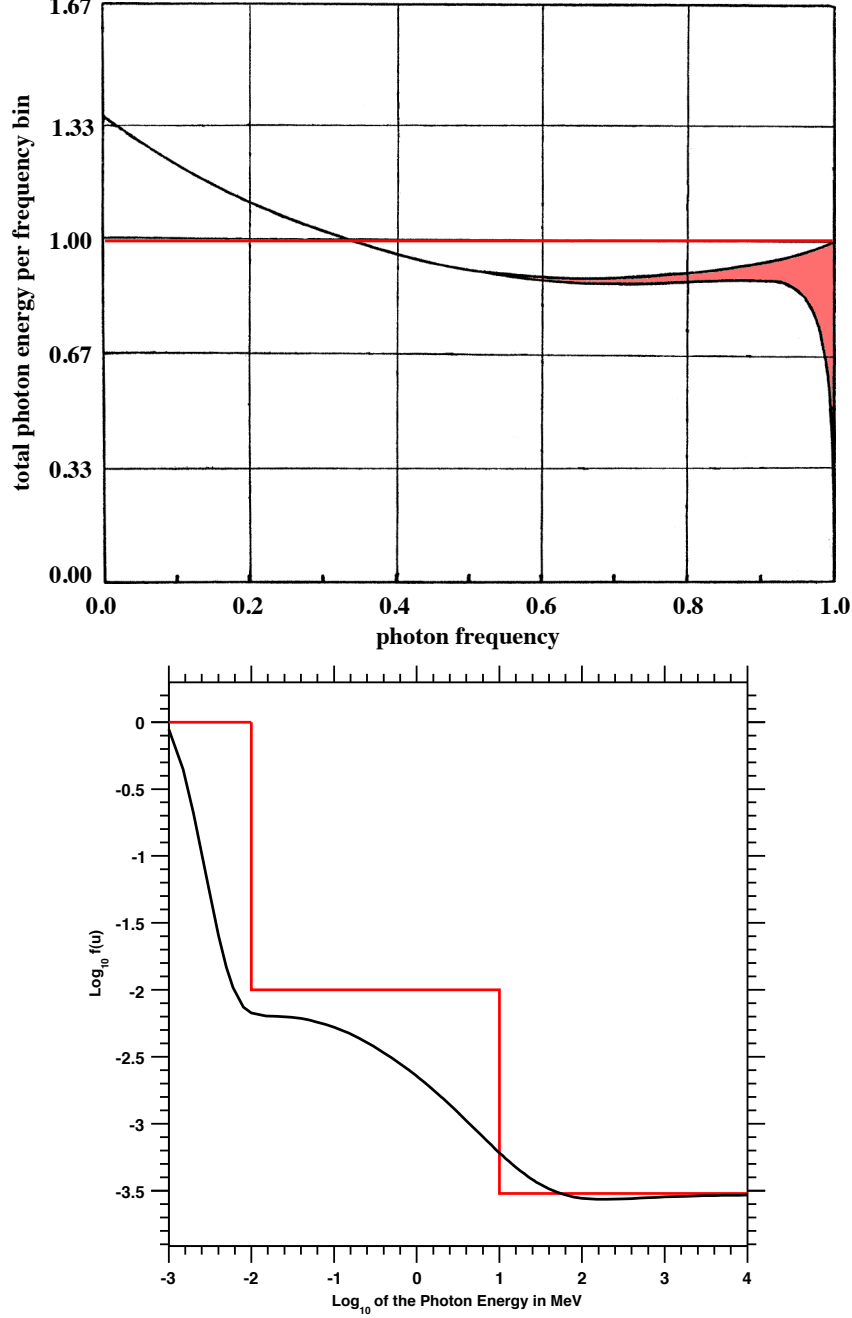
Figure 5: Upper: Bremsstrahlung Spectrum (adapted without permission from [9]). The horizontal axis is the photon frequency relative to the beam energy ($u = h\nu/E$). The vertical axis is the total photon energy per frequency bin normalized to the average value over all frequencies $\left(\frac{u}{\Phi_{\mathrm{rad}}} \left[\frac{1}{\rho} \frac{d^2\Phi(u)}{du \cdot dx} \right] \right)$. The lower bound of the pink shaded region corresponds to a beam energy of 500 MeV; while, the upper bound to the limit of infinite beam energy. In the convolution integral, Eqn. (51), this curve is taken to be independent of both u & E_{beam} and set equal to 1, which corresponds to the horizontal red line. Lower: Average Fraction of Bremsstrahlung Photons Absorbed as a Function of Photon Energy. The horizontal axis is the log base 10 of the photon energy in MeV. The vertical axis is the log base 10 of $\langle f(u) \rangle$ evaluated for a 10 amg/40 cm cell. The black curve is the true form of $\langle f(u) \rangle$ and the red curve is the rectangular approximation used for the integral Eqn. (56). In summary, the integral of Eqn. (51) is a convolution of the black curves in these two plots; whereas we approximate this integral by taking a convolution of the red curves in these plots.

12

E_i(eV)	year	comments	ref.
26.2	1925	purified in charcoal at liquid air temps, possible double ionization of He?	[14]
31	1927	purified in charcoal at liquid air temperatures	[15]
31.0	1944	value listed in [16] and [17]	[18]
29.9	1951	tank He at 99.95% purity with traces amounts of N_2 and O_2	[19]
30.9	1952	cited in [11, 20]	[21]
(32.5 ± 0.5)	1952	He/Ar/CH_4 mixture	[22]
29.7 41.3	1952	He with 0.13% Ar purified with charcoal at liquid air temperatures	[10]
(26.0 ± 1.6)	1953	was purified, but not pure enough?	[23]
$(42.7 \pm 0.2)^*$	1953	purified with charcoal at liquid air temperatures	[11]
33.8	1954	tank He with less than 0.02% N_2	[24]
$(44.2 \pm 0.9)^*$	1954	purified with Ca-Mg chips at 470ºC	[20]
$(46.0 \pm 0.5)^*$	1954	two sets of He samples with different purification methods	[12]
$(42.3 \pm 0.3)^*$	1955	purified with charcoal at liquid air temperatures	[25]
$(40.3 \pm 0.8)^*$	1956	purified with charcoal at liquid air temperatures	[26]
55,60 ($\pm$5%)	1957	used He-ethylene mix, but applied an "impurity" correction	[27]
29.9/35.2 41.1	1954	theoretical calculation for impure He sample theoretical calculation for pure He	[13]
42.7,42.3 41	1964 1994	sensitivity to impurities discussed, but no original sources listed	[28] [7]

$$E_i(\text{weighted mean}) = (43.2 \pm 0.1)\,\text{eV}$$

Table 4: Mean Energy per Ion-e^- Pair Creation in He Gas. Only measurements performed on carefully purified samples (*) are used in the calculation of the weighted mean. The different measurement techniques and their respective sensitivities to impurities are discussed in the 1958 review article by Valentine and Curran [29].

2.4 Mean Energy for Helium Ion-Electron Pair Creation

The mean energy per ion-electron creation has been measured in helium a number of times, see Tab. (4). The early measurements found about 32 eV per pair. As later authors noted on more than one occasion [10, 11, 12, 13], these early measurements were performed on insufficiently pure helium samples. Later measurements, which took great care to purify the helium sample, obtained results about 10 eV per pair higher. We use a weighted average of five "modern" measurements that went to great lengths to purify their He sample. As a side note, the mean energy per ion-electron creation E_i is entirely different than the mean excitational potential I_{BB}. It is merely a coincidence that they have nearly the same value for He. We are finally in a position to calculate the mean ionization rate per atom:

$$\Gamma_{\text{ion}} = \left(\frac{1}{eE_i} \left[\frac{1}{\rho} \frac{dE}{dx} \right]_{\text{c}} \right) \frac{I}{A_{\text{tc}}} = \beta \frac{I}{A_{\text{tc}}} \tag{60}$$

where e is the elementary charge, I is the beam current, A_{tc} is the mean cross sectional area of the target chamber, and β^{-1} is tabulated in Tab. (5) for various beam energies. The dependence of β on the beam energy is soft; consequently the mean ionization rate per atom within 5 percent over all JLab energies is:

$$\Gamma_{\text{ion}} = \left(0.01\ \frac{\text{cm}^2}{\mu\text{A} \cdot \text{hr}} \right) \frac{I}{A_{\text{tc}}} = \left(\frac{1}{20\ \text{hrs}} \right) \cdot \left(\frac{I}{10\ \mu\text{A}} \right) \cdot \left(\frac{2.0\ \text{cm}^2}{A_{\text{tc}}} \right) \tag{61}$$

E_{beam} (GeV)	$\left[\frac{1}{\rho}\frac{dE}{dx}\right]_{\text{c}}$	η (%)	β^{-1} $(\text{hr}\cdot\mu\text{A/cm}^2)$
0.5	0.963	0.06	103.8
1.0	0.982	0.10	101.9
2.0	1.000	0.17	100.0
4.0	1.018	0.31	98.19
8.0	1.037	0.58	96.45
16.0	1.055	1.11	94.77
32.0	1.074	2.16	93.15
64.0	1.092	4.22	91.58

Table 5: Variation of Ionizing Energy Loss Parameters with Electron Beam Energy. The second column is the energy lost to collisions relative to the value at 2 GeV. The maximum relative ionization contribution from radiation, η, is estimated assuming a ^{3}He density of 10 amg and a target chamber length of 40 cm.

2.5 Spin Relaxation Due to Atomic and Molecular Helium Ions

Atomic ions contribute to polarization loss due to a "spin-exchange"-like interaction between the ^{3}He nucleus and the unpaired electron in the atomic ion. Because charge exchange occurs readily, electrons from highly polarized neutral atoms jump to lowly polarized atomic ions. The newly formed atomic ion partially depolarizes until it undergoes charge exchange and so on. The cumulative effect is at most one nuclear spin flip [30]. In addition to this process, molecular ions also lose polarization to the rotational degrees of freedom via a spin-rotation interaction [31]. Little mention is made in the literature about relaxation due to interactions with free electrons, so we shall ignore them as well. Before estimating the number of spin flips induced by both processes, it is useful to first estimate the fraction of ions of both types and their typical lifetimes. First we write down the rate equations for the density of atomic ions and molecular ions (in the target chamber) assuming that most of the atoms are neutral:

$$\frac{d[\text{He}^+]_{\text{tc}}}{dt} = +\Gamma_{\text{ion}}[\text{He}]_{\text{tc}} - \sum_i k_i[X_i]_{\text{tc}}[\text{He}^+]_{\text{tc}} - k_m[\text{He}^+]_{\text{tc}}[\text{He}]_{\text{tc}}^2 + D\nabla^2[\text{He}^+]_{\text{tc}} \tag{62}$$

$$\frac{d[\text{He}_2^+]_{\text{tc}}}{dt} = +k_m[\text{He}^+]_{\text{tc}}[\text{He}]_{\text{tc}}^2 - \sum_j [X_j]_{\text{tc}}\left(k_j' + k_j''[\text{He}]_{\text{tc}}\right)[\text{He}_2^+]_{\text{tc}} + D\nabla^2[\text{He}_2^+]_{\text{tc}} \tag{63}$$

where k_m, k_i, k_j', & k_j'' are the rate constants for molecular formation, atomic ion charge transfer to X_i, binary molecular charge transfer to X_j, and three body molecular charge transfer to X_j, see Tab. (7). Losses due to diffusion can be estimated by:

$$D\nabla^2 \to \gamma_d \approx D\pi^2\left[\frac{1}{R^2} + \frac{1}{L^2}\right] \tag{64}$$

where D is the ^{3}He self-diffusion constant, R is the characteristic diffusion size in the radial direction, and L is the characteristic diffusion size along the target chamber. Using the intrinsic radius of the beam ≈ 100 μm and the target chamber length ≈ 40 cm, we get $\gamma_d \approx 200$ kHz. Since all of the other rates are on the order of GHz, we can safely ignore the effect of diffusion. In other words, the exact details of the transverse spatial distrbution of beam current is irrelevant. All that matters is the total current that passes through the target chamber. Charge recombination is assumed to be negligible. Dividing out the total ^{3}He density and assuming that N_2 is the only other gas in the target chamber, we get rate equations for the fraction of atoms ions h_a and molecular ions h_m, where we have assumed $h_a, h_m \ll 1$:

$$\frac{dh_a}{dt} = +\Gamma_{\text{ion}} - \frac{h_a}{\tau_a} \tag{65}$$

$$\tau_a^{-1} = k_n[\text{N}_2]_{\text{tc}} + k_m[\text{He}]_{\text{tc}}^2 \tag{66}$$

$$\frac{dh_m}{dt} = +k_m h_a[\text{He}]_{\text{tc}}^2 - \frac{h_m}{\tau_m} \tag{67}$$

14

parameter	value	units	description
$[\mathrm{He}]_{\mathrm{tc}}$	10	amg	operating target chamber density
$[\mathrm{N_2}]_{\mathrm{tc}}$	0.1	amg	operating target chamber density
ρ	1	-	ratio of $\mathrm{N_2}$ to $^3\mathrm{He}$ densities relative to 0.01
h	1.0	-	density of $^3\mathrm{He}$ relative to 10 amg
I	10	$\mu\mathrm{A}$	beam current
A_{tc}	2	cm^2	target chamber cross sectional area
Γ_{ion}	1/20	hrs^{-1}	ionization rate per atom
D	1.8	cm^2/s	$^3\mathrm{He}$ self-diffusion constant at STP
$k_m[\mathrm{He}]_{\mathrm{tc}}^2$	6.0	GHz	molecular ion formation rate
$k_n[\mathrm{N_2}]_{\mathrm{tc}}$	2.7	GHz	atomic ion rate of charge transfer to $\mathrm{N_2}$
$k_n'[\mathrm{N_2}]_{\mathrm{tc}}$	3.0	GHz	molceular ion binary rate of charge transfer to $\mathrm{N_2}$
$k_n''[\mathrm{N_2}]_{\mathrm{tc}}[\mathrm{He}]_{\mathrm{tc}}$	9.8	GHz	molecular ion 3-body rate of charge transfer to $\mathrm{N_2}$
τ_a	115	ps	mean lifetime of atomic ions
τ_m	78	ps	mean lifetime of molecular ions
τ_{ex}	6.7	ps	mean time between atomic charge transfers
h_a^∞	1.5×10^{-15}	-	fraction of nuclei that are in atomic ions
h_m^∞	7.2×10^{-16}	-	fraction of nuclei that are in molecular ions
A_a/h	8.66	GHz	atomic ion hyperfine coupling constant [30]
$\gamma_m N/h$	29	MHz	molecular ion spin-rotation coupling constant [31]
Q_m	≤ 1	-	relative molecular ion relexation rate
n_m	≤ 0.002	-	spin flips due to molecular ions per atomic ion created
Ω	0.36	radians	amount of nuclear spin precession in between charge transfers
r	17	-	mean number of atomic charge transfers before neutralization
n_a	0.50 ± 0.07	-	spin flips due to atomic ions per atomic ion created

Table 6: Parameters Relevant to Relaxation Due to Ion Formation. These values are calculated for typical operating conditions.

reaction	type	binary	3-body	ref
$He^+ + He \rightarrow He + He^+$	charge exchange	15 ± 5	-	[32]
$He^+ + N_2 \rightarrow He + N_2^+$ $He^+ + O_2 \rightarrow He + O_2^+$	charge transfer	27 ± 8 23 ± 7	- -	[33]
$He^+ + 2He \rightarrow He + He_2^+$	molecular formation	-	0.060 ± 0.012	[34]
$He_2^+ + He \rightarrow He + He_2^+$	charge exchange	6 ± 3	-	[31]
$He_2^+ + CO_2 \rightarrow 2He + CO_2^+$	charge transfer	48 ± 13	-	[35]
$He_2^+ + (0,1)He + N_2 \rightarrow (2,3)He + N_2^+$	charge transfer	30 ± 3	9.8 ± 1.4	[36]
$He_2^+ + (0,1)He + H_2 \rightarrow (2,3)He + H_2^+$ $He_2^+ + (0,1)He + H_2O \rightarrow (2,3)He + H_2O^+$ $He_2^+ + (0,1)He + O_2 \rightarrow (2,3)He + O_2^+$	charge transfer	11 ± 3 22 ± 11 27 ± 8	6.5 ± 3.6 87 ± 18 25 ± 7	[37]

Table 7: Atomic and Molecular Ion Reaction Rate Constants. Binary rate constants are in GHz/amg and 3-body rate constants are in GHz/amg^2. All values are assumed to be measured at 300 K and to have neglible temperature dependence within the quoted uncertainties.

$$\tau_m^{-1} \quad = \quad [N_2]_{tc} \left(k_n' + k_n''[He]_{tc} \right) \tag{68}$$

where τ_a and τ_m are the mean atomic and molecular ion lifetimes. The equilibrium fractions are obtained from setting the rates to zero and give:

$$h_a^\infty \quad = \quad \Gamma_{ion}\tau_a = \frac{\Gamma_{ion}}{k_n[N_2]_{tc} + k_m[He]_{tc}^2} \tag{69}$$

$$h_m^\infty \quad = \quad k_m[He]_{tc}^2 \tau_m h_a^\infty = \frac{\Gamma_{ion}}{[N_2]_{tc}\left(k_n' + k_n''[He]_{tc}\right)} \left(1 + \frac{k_n[N_2]_{tc}}{k_m[He]_{tc}^2}\right)^{-1} \tag{70}$$

Under our conditions, we find $\tau_a, \tau_m \approx 100$ ps and $h_a^\infty, h_m^\infty \approx 10^{-15}$, which justifies our previous assumption that there are very few ions.

The presence of a foreign gas such as N_2 greatly limits the lifetime of molecular ions. Whereas molecular ions have the potential to depolarize many nuclei, their effect is greatly reduced because they are so short lived. Relaxation due to molecular ions is discussed in [31] and they derive an expression for n_m of the following form:

$$\Gamma_{ion}n_m = \left\langle \frac{\gamma_m N}{h} \right\rangle h_m^\infty Q_m \rightarrow n_m = \left\langle \frac{\gamma_m N}{h} \right\rangle \left(\frac{h_m^\infty}{\Gamma_{ion}}\right) Q_m \tag{71}$$

where $\gamma_m N/h$ is the molecular spin-rotation coupling constant and Q_m is the unitless relative relaxation rate that depends on the magnitude of the magnetic fields and the density of ^{3}He. Since Q_m can be at most 1, the maximum value for n_m is given as:

$$n_m \leq \frac{\left\langle \frac{\gamma_m N}{h} \right\rangle}{[N_2]_{tc}\left(k_n' + k_n''[He]_{tc}\right)} \left(1 + \frac{k_n[N_2]_{tc}}{k_m[He]_{tc}^2}\right)^{-1} \approx 0.002 \tag{72}$$

Relaxation due to atomic ions is discussed in [30] and their calculation gives:

$$n_a(r,\Omega) \quad = \quad 1 + \frac{a_1}{1 - r\gamma_1} + \Re\left(\frac{a_2}{1 - r\gamma_2}\right)$$

$$
\begin{aligned}
a_1 &= \frac{-|\gamma_2|^2 + \Omega^2/2}{|\gamma_2|^2 + 2\gamma_1\,(1+\gamma_1)} \\[4pt]
a_2 &= \frac{2\left(\Omega^2/2 - \gamma_1\gamma_2^*\right)\left(\gamma_1 - \gamma_2^*\right)}{(\gamma_2^* - \gamma_2)\left[|\gamma_2|^2 + 2\gamma_1\,(1+\gamma_1)\right]} \\[4pt]
\gamma_1 &= S + T - \frac{2}{3} \\[4pt]
\gamma_2 &= \left(\frac{i\sqrt{3}-1}{2}\right)S - \left(\frac{i\sqrt{3}+1}{2}\right)T - \frac{2}{3} \\[4pt]
S &= (Q+R)^{1/3} \\[4pt]
T &= (Q-R)^{1/3} \\[4pt]
Q &= \frac{1}{108}\left(4 + 9\Omega^2\right) \\[4pt]
R &= \frac{\Omega}{12\sqrt{3}}\left(8 - 13\Omega^2 + 16\Omega^4\right)^{1/2} \\[4pt]
\Omega &= 2\pi\left(\frac{A_a}{h}\right)\tau_{\mathrm{ex}} \\[4pt]
r &= \frac{\tau_{\mathrm{a}}}{\tau_{\mathrm{ex}}}
\end{aligned}
\tag{73}
$$

where τ_{ex} is the mean time between atomic charge exchange collisions, A_a/h is the atomic ion hyperfine coupling constant, r is the mean number of charge exchange collisions before the atomic ion is neutralized, and Ω is a measure of "how much" the nuclear spin and unpaired electron interact before a charge exchange collision occurs. Note that since Q and R are positive definite, γ_1 and a_1 are necessarily be real and we can and must choose T to be real as well.

Fig. (6) depicts n_a for various values of r, Ω, ^{3}He density, and N_2 to ^{3}He density ratio. The red point in the left plot corresponds to our typical conditions with $n_a = 0.50 \pm 0.07$, where all of the uncertainty comes from our (lack of) knowledge of the atomic charge transfer and molecular formation rate constants. It is quite tedious to calculate n_a directly from the above set of equations. Therefore we have prepared a "homemade" parameterization in matrix form which reproduces the full calculation of n_a to better than 0.5% for ^{3}He densities from 7 to 14 amg ($h = [^3\mathrm{He}]_{\mathrm{tc}}/10$ amg) with N_2 to ^{3}He density ratios ($\rho \equiv 100 \cdot [N_2]_{\mathrm{tc}}/[^3\mathrm{He}]_{\mathrm{tc}}$) from 1/3% to 3%:

$$
n_a\left(h,\rho\right) =
\begin{bmatrix} 1 \\ h \\ h^2 \\ h^3 \end{bmatrix}^{\mathrm{T}}
\begin{bmatrix}
+1.0283\mathrm{E}{+}0 & +2.2063\mathrm{E}{-}1 & -5.4940\mathrm{E}{-}2 & +4.9159\mathrm{E}{-}3 \\
+1.9515\mathrm{E}{-}1 & -9.0280\mathrm{E}{-}1 & +1.6384\mathrm{E}{-}1 & -1.2999\mathrm{E}{-}2 \\
-9.8146\mathrm{E}{-}1 & +7.6918\mathrm{E}{-}1 & -1.1821\mathrm{E}{-}1 & +8.0086\mathrm{E}{-}3 \\
+3.5643\mathrm{E}{-}1 & -1.9663\mathrm{E}{-}1 & +2.5395\mathrm{E}{-}2 & -1.2960\mathrm{E}{-}3
\end{bmatrix}
\begin{bmatrix} 1 \\ \rho \\ \rho^2 \\ \rho^3 \end{bmatrix}
\tag{74}
$$

where, to reiterate:

$$
h = \frac{[^3\mathrm{He}]_{\mathrm{tc}}}{10 \text{ amg}} \qquad \& \qquad \rho = 100 \cdot \frac{[N_2]_{\mathrm{tc}}}{[^3\mathrm{He}]_{\mathrm{tc}}}
\tag{75}
$$

The right half of Fig. (6) shows a comparison between the full calculation for n_a and the matrix parameterization as a functon of ^{3}He density for different N_2 to ^{3}He density ratios. The desired amount of N_2 in the cell is usually about one percent or $\rho = 1$. In this case, the matrix form of n_a collapses to give:

$$
n_a\left(h, \rho = 1\right) = 1.1989 - 0.55681 \cdot h - 0.32248 \cdot h^2 + 0.18390 \cdot h^3
\tag{76}
$$

If the ^{3}He density is 10 amg or $h = 1$, the the matrix collapses to give:

$$
n_a\left(h = 1, \rho\right) = 0.59842 - 0.10962 \cdot \rho + 0.016085 \cdot \rho^2 - 0.0013705 \cdot \rho^3
\tag{77}
$$
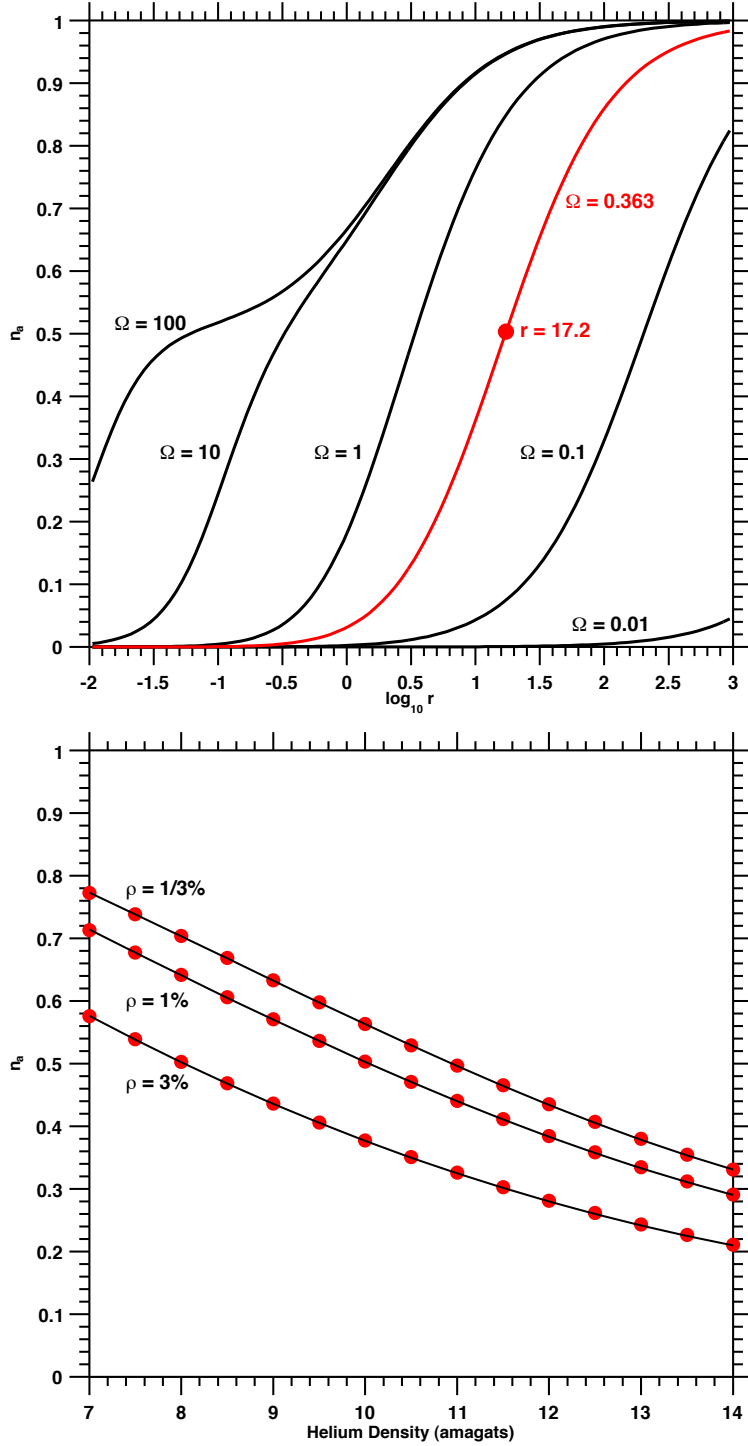
Figure 6: Mean Number of Spin Flips Due to Atomic Ions. Upper: n_a as function of r and Ω. This is a recreation of Fig. (1) from [30] with the addition of the red curve which corresponds to a ^{3}He density of 10 amg. The red point corresponds to values for n_a and r when the N_2 to ^{3}He density (ρ) is 1%. Lower: n_a as a function of ^{3}He density for three different values of ρ. The red points are obtained from the full calculation, Eqs. (73); whereas the black curves are obtained from the matrix parameterization, Eq. (74). This parameterization reproduces the full calculation to better than half a percent over ($0.7 \le h \le 1.4$) and ($1/3 \le \rho \le 3$). Note that increasing the relative density of N_2 helps suppress n_a.

3 Polarization Diffusion

3.1 Diffusion Rate Per Atom

The flux of particles $\vec{J}$ of the ith type due to diffusion is [38]:

$$\vec{J}_i = -nD\left[\vec{\nabla}f_i - k_T\log(T) - k_p\log(p)\right] \tag{78}$$

where f_i is the fraction of particles of the ith particle type such that $\sum_i f_i = 1$, D is the diffusion constant, $k_{T(p)}$ is the thermal diffusion (barodiffusion) ratio, n is the total density of particles, and $T(p)$ is the temperature (pressure) of the gas. Reducing the problem to one dimension $\left(\vec{\nabla}\to\hat{z}\frac{d}{dz}\right)$, labeling i as the up and down spins, and subtracting one from the other gives us the net polarization flux through the transfer tube:

$$J_{\mathrm{tt}} = \hat{z}\cdot\left(\vec{J}_+ - \vec{J}_-\right) = -n(z)D(z)\hat{z}\cdot\vec{\nabla}\left(f_+ - f_-\right) = -n(z)D(z)\frac{dP(z)}{dz} \tag{79}$$

Note that we have assumed that the diffusion ratios k_T and k_p depend only on the type of chemical species and not on the specific spin state. To solve this equation for J_{tt}, we'll make the assumption that J_{tt} is constant, $\frac{dJ_{\mathrm{tt}}}{dz}\approx 0$, and that there is a linear temperature gradient between the two chambers [39]. The temperature dependence of the diffusion constant can be seen by considering the diffusion relation for a classical gas of hard spheres:

$$D = \frac{\bar{v}l_{\mathrm{mfp}}}{3} = \sqrt{\frac{8RT}{\pi M}}\frac{1}{3n\sigma} = D_0\sqrt{\frac{T}{T_0}}\left(\frac{n_0}{n}\right)\left(\frac{\sigma_0}{\sigma}\right) = D_0\left(\frac{T}{T_0}\right)^{m-1}\left(\frac{n_0}{n}\right) = D_0\left(\frac{T}{T_0}\right)^m \tag{80}$$

where $\bar{v}$ is the mean thermal velocity, l_{mfp} is the mean free path, n is the gas density, and σ is the collisional cross section. At constant pressure, the density has an inverse temperature dependence and the cross section has some temperature dependence that has to be determined empiracally:

$$m = \frac{1}{2}\text{ (from the velocity)} + 1\text{ (from the density)} + m_\sigma\text{ (from the cross section)} \tag{81}$$

Using this form of the diffusion constant, moving some things around, and integrating along the transfer tube length gives:

$$J_{\mathrm{tt}} = -n(z)D_0\left(\frac{T}{T_0}\right)^{m-1}\frac{n_0}{n(z)}\frac{dP(z)}{dz}$$

$$-\frac{J_{\mathrm{tt}}T_0^{m-1}}{D_0 n_0}\int_0^{L_{\mathrm{tt}}}T(z)^{1-m}\,dz = \int_0^{L_{\mathrm{tt}}}\frac{dP(z)}{dz}dz$$

$$-\frac{J_{\mathrm{tt}}T_0^{m-1}}{D_0 n_0}\frac{L_{\mathrm{tt}}}{T_{\mathrm{pc}}-T_{\mathrm{tc}}}\int_{T_{\mathrm{tc}}}^{T_{\mathrm{pc}}}u^{1-m}\,du = P(L_{\mathrm{tt}}) - P(0)$$

$$-\frac{J_{\mathrm{tt}}T_0^{m-1}}{D_0 n_0}\frac{L_{\mathrm{tt}}}{T_{\mathrm{pc}}-T_{\mathrm{tc}}}\left(\frac{T_{\mathrm{pc}}^{2-m}-T_{\mathrm{tc}}^{2-m}}{2-m}\right) = P_{\mathrm{pc}} - P_{\mathrm{tc}} \tag{82}$$

Finally solving for J_{tt} gives:

$$J_{\mathrm{tt}} = -\left(P_{\mathrm{pc}}-P_{\mathrm{tc}}\right)\left[D_0\left(\frac{T_{\mathrm{tc}}}{T_0}\right)^{m-1}\frac{n_0}{n_{\mathrm{tc}}}\right]\frac{n_{\mathrm{tc}}}{L_{\mathrm{tt}}}\frac{(2-m)(t-1)}{(t^{2-m}-1)}\quad\&\quad t = \frac{T_{\mathrm{pc}}}{T_{\mathrm{tc}}} \tag{83}$$

where D_0 is the diffusion constant at a reference temperature T_0 and density n_0 listed in Tab. (8), T_{tc} & n_{tc} are the temperature and density of the target chamber, and t is the ratio of the pumping chamber to target chamber temperature. Note that J_{tt} is the total rate per unit area, whereas we want the rate per

parameter	value	units
D_0	2.79	cm^2/s
T_0	353	K
n_0	0.773	amg
m	1.70	-

Table 8: ^{3}He Self-Diffusion Constant Parameters from [40].

atom. Multiplying by the transfer tube cross sectional area A_{tt}, dividing by the number of particles in each chamber, and comparing to Eqns. (7) & (8) give the following relations for the diffusion rates per atom:

$$
\begin{aligned}
d_{\text{pc}} &= -\frac{J_{\text{tt}} A_{\text{tt}}}{V_{\text{pc}} n_{\text{pc}} \left(P_{\text{pc}} - P_{\text{tc}}\right)} = \frac{A_{\text{tt}}}{V_{\text{pc}} L_{\text{tt}}} \left[D_0 \left(\frac{T_{\text{pc}}}{T_0}\right)^{m-1} \frac{n_0}{n_{\text{pc}}} \right] \frac{(2-m)\left(1-t^{-1}\right)}{\left(1-t^{m-2}\right)} \\
d_{\text{tc}} &= -\frac{J_{\text{tt}} A_{\text{tt}}}{V_{\text{tc}} n_{\text{tc}} \left(P_{\text{pc}} - P_{\text{tc}}\right)} = \frac{A_{\text{tt}}}{V_{\text{tc}} L_{\text{tt}}} \left[D_0 \left(\frac{T_{\text{tc}}}{T_0}\right)^{m-1} \frac{n_0}{n_{\text{tc}}} \right] \frac{(2-m)(t-1)}{\left(t^{2-m}-1\right)}
\end{aligned}
\tag{84}
$$

where we have made use of the following identity:

$$
\left[\left(\frac{T_{\text{pc}}}{T_0}\right)^{m-1}\right] \frac{\left(1-t^{-1}\right)}{\left(1-t^{m-2}\right)} = \left[\left(\frac{T_{\text{tc}}}{T_0}\right)^{m-1}\right] \frac{(t-1)}{\left(t^{2-m}-1\right)}
\tag{85}
$$

Note that the pumping chamber and target chamber operating densities are related by:

$$
n_{\text{pc}} = \frac{n_{\text{tc}}}{t} = n_{\text{fill}} \left(\frac{1+v}{t+v}\right) \quad \& \quad v = \frac{V_{\text{pc}}}{V_{\text{tc}}} \quad \& \quad t = \frac{T_{\text{pc}}}{T_{\text{tc}}}
\tag{86}
$$

where v is the ratio of the pumping chamber volume to the target chamber volume and we have tacitly assumed that the fraction of nuclei in the transfer tube is negligible. Combining this relation with Eqns. (84) & (3) gives:

$$
f_{\text{pc}} = \frac{v}{t+v}
\tag{87}
$$

$$
f_{\text{tc}} = \frac{t}{t+v}
\tag{88}
$$

$$
d_{\text{pc}} = \left(\frac{t}{v}\right) d_{\text{tc}}
\tag{89}
$$

$$
d_{\text{tc}} = \frac{A_{\text{tt}}}{V_{\text{tc}} L_{\text{tt}} n_{\text{fill}}} \left[D_0 n_0 \left(\frac{273.15\ \text{K}}{T_0}\right)^{m-1} \right] \frac{(t+v)(2-m)(t-1)}{t(1+v)\left(t^{2-m}-1\right)} \left(\frac{T_{\text{tc}}}{273.15\ \text{K}}\right)^{m-1}
\tag{90}
$$

where:

$$
\left[D_0 n_0 \left(\frac{273.15\ \text{K}}{T_0}\right)^{m-1} \right] = 6488.21\ \frac{\text{cm}^2 \cdot \text{amg}}{\text{hr}}
\tag{91}
$$

The diffusion rate out of the target chamber per atom can be alternatively written as:

$$
\begin{aligned}
d_{\text{tc}} &= \left(0.60\ \text{hr}^{-1}\right) \left(\frac{A_{\text{tt}}}{0.5\ \text{cm}^2}\right) \left(\frac{6\ \text{cm}}{L_{\text{tt}}}\right) \left(\frac{90\ \text{cm}^3}{V_{\text{tc}}}\right) \left(\frac{10\ \text{amg}}{n_{\text{tc}}}\right) \left(\frac{0.3t - 0.3}{t^{0.3} - 1}\right) \left(\frac{T_{\text{tc}}}{273.15\ \text{K}}\right)^{0.7} \\
&= \left(0.80\ \text{hrs}^{-1}\right) \left(\frac{A_{\text{tt}}}{0.5\ \text{cm}^2}\right) \left(\frac{6\ \text{cm}}{L_{\text{tt}}}\right) \left(\frac{90\ \text{cm}^3}{V_{\text{tc}}}\right) \left(\frac{10\ \text{amg}}{n_{\text{tc}}}\right) \left(\frac{\Upsilon\left(T_{\text{pc}}, T_{\text{tc}}\right)}{4/3}\right)
\end{aligned}
\tag{92, 93}
$$

$$
\Upsilon\left(T_{\text{pc}}, T_{\text{tc}}\right) = 0.3 \left(\frac{t-1}{t^{0.3} - 1}\right) \left(\frac{T_{\text{tc}}}{273.15\ \text{K}}\right)^{0.7}
\tag{94}
$$

20

where Υ is a dimensionless factor, usually between 1.2 and 1.5, that depends only on the cell temperatures. Note that when the cell is at a uniform temperature, $T_{\text{pc}} = T_{\text{tc}}$:

$$\lim_{t \to 1} \Upsilon = \lim_{t \to 1} 0.3 \left(\frac{t-1}{t^{0.3}-1} \right) \left(\frac{T_{\text{tc}}}{273.15 \text{ K}} \right)^{0.7} = \lim_{t \to 1} 0.3 \left(\frac{1}{0.3} \right) \left(\frac{T_{\text{tc}}}{273.15 \text{ K}} \right)^{0.7} = \left(\frac{T_{\text{tc}}}{273.15 \text{ K}} \right)^{0.7} \tag{95}$$

3.2 Depolarization Within the Transfer Tube

Thus far we have neglected the polarization dynamics in the transfer tube since only a small fraction of ^{3}He nuclei are in the transfer tube volume. In this section, we will estimate the size of the correction needed to account for spin relaxation in the transfer tube. First we need to estimate the fraction of nuclei in the transfer tube volume. This is obtained from an integral over the transfer tube length:

$$f_{\text{tt}} = \frac{N_{\text{tt}}}{N_{\text{tot}}} = \frac{A_{\text{tt}}}{n_{\text{fill}} V_{\text{tot}}} \int_0^{L_{\text{tt}}} n_{\text{tt}}(z) \ dz \tag{96}$$

Assuming a linear temperature gradient with one end being at the pumping chamber temperature and the other end being at the target chamber temperature:

$$T(z) = T_{\text{pc}} + (T_{\text{tc}} - T_{\text{pc}}) \frac{z}{L_{\text{tt}}} \tag{97}$$

gives the following equivalent integral over temperature:

$$f_{\text{tt}} = \frac{V_{\text{tt}}}{n_{\text{fill}} V_{\text{tot}}} \frac{P}{R \left(T_{\text{tc}} - T_{\text{pc}} \right)} \int_{T_{\text{pc}}}^{T_{\text{tc}}} \frac{dT}{T} \tag{98}$$

Rewriting in terms of densities gives:

$$f_{\text{tt}} = \frac{V_{\text{tt}}}{V_{\text{tot}}} \left[\frac{n_{\text{fill}}}{n_{\text{pc}}} - \frac{n_{\text{fill}}}{n_{\text{tc}}} \right]^{-1} \log \left(\frac{n_{\text{tc}}}{n_{\text{pc}}} \right) \tag{99}$$

If we make the assumption that $f_{\text{tt}} \ll 1$, then we can use Eq. (86) and $f_{\text{pc}}/f_{\text{tc}} = v/t$ to get:

$$f_{\text{tt}} = \frac{V_{\text{tt}}}{V_{\text{tc}}} \frac{\log(t)}{\left(1 + f_{\text{pc}}/f_{\text{tc}} \right) \left(t - 1 \right)} \tag{100}$$

Under typical conditions, $t = 1.7$, $f_{\text{pc}}/f_{\text{tc}}$ varies very roughly from 1 to 2, $V_{\text{tt}} = 4$ cc, and $V_{\text{tc}} = 90$ cc, which gives $f_{\text{tt}} \leq 0.02$. This justifies our approximation that the fraction of nuclei in the transfer tube is very small.

Next, we'll model the transfer tube as a virtual "chamber" somewhere between the pumping and target chambers. The spin relaxation that occurs throughout the physical transfer tube will be averaged to find the equivalent spin relaxation in this virtual chamber. Under these assumptions, it is straightforward to generalize the two chamber polarization rate equations, Eq. (6), into three chamber polarization rate equations:

$$\frac{dP_{\text{pc}}}{dt} = \gamma_{\text{se}} \left(P_A - P_{\text{pc}} \right) - \Gamma_{\text{pc}} P_{\text{pc}} - d_{\text{pc}}^{\text{tt}} \left(P_{\text{pc}} - P_{\text{tt}} \right) \tag{101}$$

$$\frac{dP_{\text{tt}}}{dt} = -\Gamma_{\text{tt}} P_{\text{tt}} - d_{\text{tt}}^{\text{pc}} \left(P_{\text{tt}} - P_{\text{pc}} \right) - d_{\text{tt}}^{\text{tc}} \left(P_{\text{tt}} - P_{\text{tc}} \right) \tag{102}$$

$$\frac{dP_{\text{tc}}}{dt} = d_{\text{tc}}^{\text{tt}} \left(P_{\text{tt}} - P_{\text{tc}} \right) - \Gamma_{\text{tc}} P_{\text{tc}} \tag{103}$$

where P_{tt} is the effective transfer tube polarization and Γ_{tt} is the average transfer tube relaxation rate. Note that we now have four diffusion rates which correspond to diffusion from the pumping and target chambers into the virtual chamber and vice versa. At nuclei number equilibrium, they must satisfy:

$$f_{\text{pc}} d_{\text{pc}}^{\text{tt}} = f_{\text{tt}} d_{\text{tt}}^{\text{pc}} \qquad \& \qquad f_{\text{tc}} d_{\text{tc}}^{\text{tt}} = f_{\text{tt}} d_{\text{tt}}^{\text{tc}} \tag{104}$$
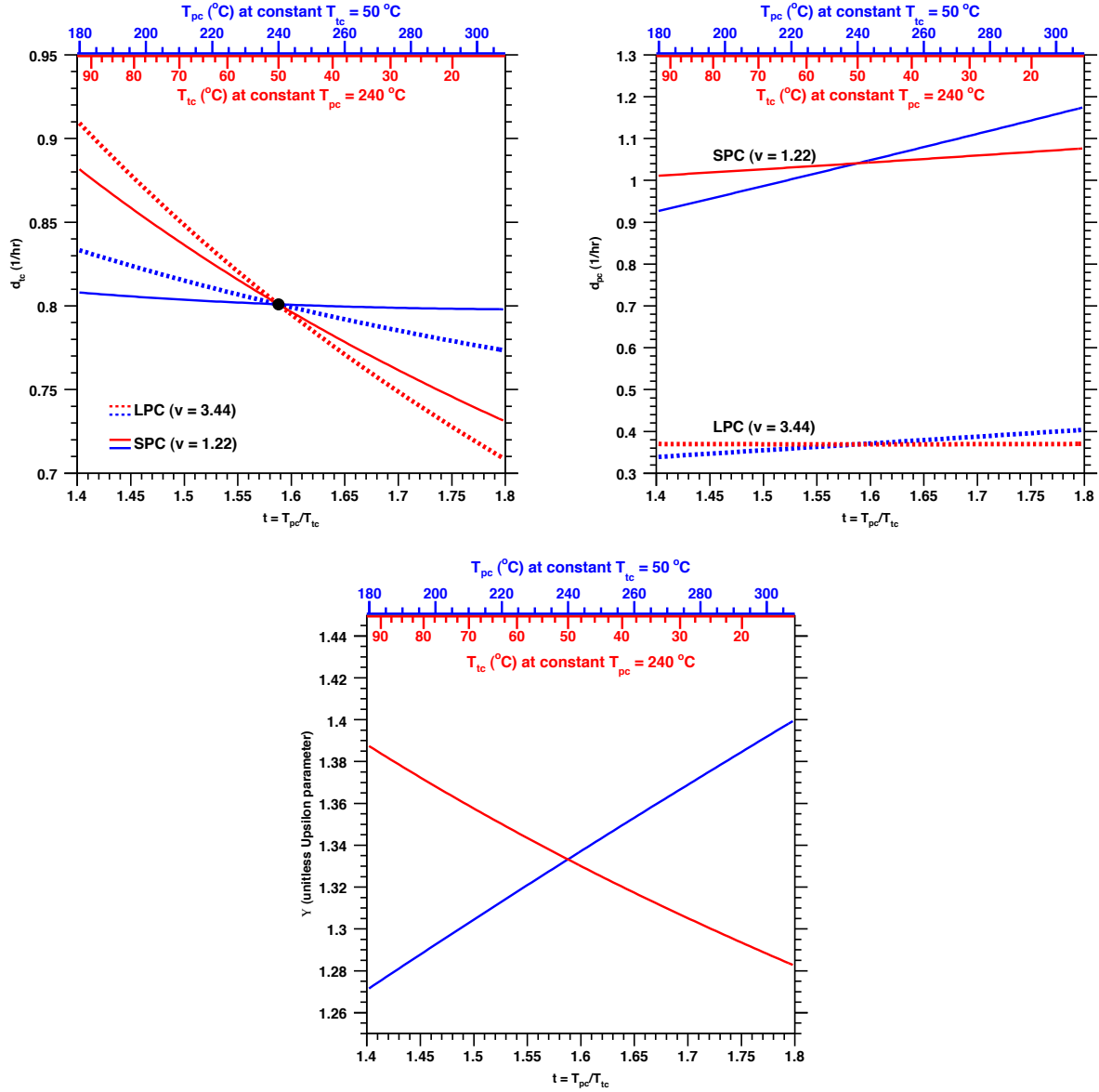
Figure 7: Diffusion Rates per Nuclei As a Function of Temperature. Upper Left: d_{tc} as function of temperatures. Upper Right: d_{pc} as a function of temperatures. Lower: Unitless temperature parameter $\Upsilon(t, T_{tc})$ as a function of temperature. Solid curves are for SPC (small pumping chamber cells), whereas dotted curves are for LPC (large pumping chamber cells). Only the volume ratio v is varied between the SPC and LPC curves with all else being equal. The blue curves and axis represent varying pumping chamber temperatures for a constant target chamber temperature. The red curves and axis represent varying target chamber temperatures for a constant pumping chamber temperature.

where the subscripts and superscripts on d refer to the source and destination chambers respectively. At equilibrium, the polarizations in the three chambers are:

$$\frac{P_{\text{tc}}^\infty}{P_{\text{tt}}^\infty} = \left[1 + \frac{\Gamma_{\text{tc}}}{d_{\text{tc}}^{\text{tt}}}\right]^{-1} \tag{105}$$

$$\frac{P_{\text{tt}}^\infty}{P_{\text{pc}}^\infty} = \left[1 + \frac{\Gamma_{\text{tt}}}{d_{\text{tt}}^{\text{pc}}} + \left(\frac{\Gamma_{\text{tc}}}{d_{\text{tc}}^{\text{tt}}}\right)\left(\frac{d_{\text{tt}}^{\text{tc}}}{d_{\text{tt}}^{\text{pc}}}\right)\left(1 + \frac{\Gamma_{\text{tc}}}{d_{\text{tc}}^{\text{tt}}}\right)^{-1}\right]^{-1} \tag{106}$$

$$\frac{P_{\text{pc}}^\infty}{P_A} = \left[1 + \frac{\Gamma_{\text{pc}}}{\gamma_{\text{se}}} + \frac{d_{\text{pc}}^{\text{tt}}}{\gamma_{\text{se}}}\left(\frac{\Gamma_{\text{tt}}}{d_{\text{tt}}^{\text{pc}}}\left[1 + \frac{\Gamma_{\text{tc}}}{d_{\text{tc}}^{\text{tt}}}\right] + \frac{\Gamma_{\text{tc}}}{d_{\text{tc}}^{\text{tt}}}\frac{d_{\text{tt}}^{\text{tc}}}{d_{\text{tt}}^{\text{pc}}}\right)\left(\left[1 + \frac{\Gamma_{\text{tt}}}{d_{\text{tt}}^{\text{pc}}}\right]\left[1 + \frac{\Gamma_{\text{tc}}}{d_{\text{tc}}^{\text{tt}}}\right] + \frac{\Gamma_{\text{tc}}}{d_{\text{tc}}^{\text{tt}}}\frac{d_{\text{tt}}^{\text{tc}}}{d_{\text{tt}}^{\text{pc}}}\right)^{-1}\right]^{-1} \tag{107}$$

If we assume that the system is at nuclei number equilibrium, then we can use Eq. (104) to write these equilibrium polarizations in a more illuminating form:

$$P_{\text{pc}}^\infty = \frac{P_A \gamma_{\text{se}} f_{\text{pc}}}{\gamma_{\text{se}} f_{\text{pc}} + \Gamma_{\text{pc}} f_{\text{pc}} + \left[\left(1 + \frac{\Gamma_{\text{tc}}}{d_{\text{tc}}^{\text{tt}}}\right)\Gamma_{\text{tt}} f_{\text{tt}} + \Gamma_{\text{tc}} f_{\text{tc}}\right]\left[1 + \Gamma_{\text{tc}} f_{\text{tc}}\left(\frac{1}{f_{\text{tc}} d_{\text{tc}}^{\text{tt}}} + \frac{1}{f_{\text{pc}} d_{\text{pc}}^{\text{tt}}}\right) + \left(1 + \frac{\Gamma_{\text{tc}}}{d_{\text{tc}}^{\text{tt}}}\right)\frac{f_{\text{tt}}}{f_{\text{pc}}}\frac{\Gamma_{\text{tt}}}{d_{\text{pc}}^{\text{tt}}}\right]^{-1}} \tag{108}$$

$$\frac{P_{\text{tc}}^\infty}{P_{\text{pc}}^\infty} = \left[1 + \Gamma_{\text{tc}} f_{\text{tc}}\left(\frac{1}{f_{\text{tc}} d_{\text{tc}}^{\text{tt}}} + \frac{1}{f_{\text{pc}} d_{\text{pc}}^{\text{tt}}}\right) + \left(1 + \frac{\Gamma_{\text{tc}}}{d_{\text{tc}}^{\text{tt}}}\right)\left(\frac{f_{\text{tt}}}{f_{\text{pc}}}\right)\left(\frac{\Gamma_{\text{tt}}}{d_{\text{pc}}^{\text{tt}}}\right)\right]^{-1} \tag{109}$$

In the limit that the diffusion rates approach infinity, $d_{\text{pc}}^{\text{tt}}, d_{\text{tc}}^{\text{tt}} \to \infty$, the above equations reduce to a very satisfying result:

$$\frac{P_{\text{tc}}^\infty}{P_{\text{pc}}^\infty} \to 1 \qquad \& \qquad P_{\text{pc}}^\infty \to P_A \frac{\gamma_{\text{se}} f_{\text{pc}}}{\gamma_{\text{se}} f_{\text{pc}} + \Gamma_{\text{pc}} f_{\text{pc}} + \Gamma_{\text{tt}} f_{\text{tt}} + \Gamma_{\text{tc}} f_{\text{tc}}} = P_A \frac{\langle\gamma_{\text{se}}\rangle}{\langle\gamma_{\text{se}}\rangle + \langle\Gamma\rangle} \tag{110}$$

In the limit that the fraction of nuclei in the transfer tube approaches zero, $f_{\text{tt}} \to 0$, the three chamber equilibrium polarization equations reduce to the familiar two chamber results, Eqs. (17) & (18):

$$P_{\text{pc}}^\infty = \frac{P_A \gamma_{\text{se}} f_{\text{pc}}}{\gamma_{\text{se}} f_{\text{pc}} + \Gamma_{\text{pc}} f_{\text{pc}} + \Gamma_{\text{tc}} f_{\text{tc}}\left[1 + \Gamma_{\text{tc}} f_{\text{tc}}\left(\frac{1}{f_{\text{tc}} d_{\text{tc}}^{\text{tt}}} + \frac{1}{f_{\text{pc}} d_{\text{pc}}^{\text{tt}}}\right)\right]^{-1}} \tag{111}$$

$$\frac{P_{\text{tc}}^\infty}{P_{\text{pc}}^\infty} = \left[1 + \Gamma_{\text{tc}} f_{\text{tc}}\left(\frac{1}{f_{\text{tc}} d_{\text{tc}}^{\text{tt}}} + \frac{1}{f_{\text{pc}} d_{\text{pc}}^{\text{tt}}}\right)\right]^{-1} \tag{112}$$

To make this reduction manifest, note our prior assumption that the nuclei flux is constant throughout the transfer tube:

$$J_{\text{tt}} = \text{constant} = \frac{d_{\text{tc}} N_{\text{tc}}}{A_{\text{tt}}}\left(P_{\text{pc}} - P_{\text{tc}}\right) = \frac{d_{\text{tc}}^{\text{tt}} N_{\text{tc}}}{A_{\text{tt}}}\left(P_{\text{tt}} - P_{\text{tc}}\right) = \frac{d_{\text{pc}}^{\text{tt}} N_{\text{pc}}}{A_{\text{tt}}}\left(P_{\text{pc}} - P_{\text{tt}}\right) \tag{113}$$

If, in addition to the above identities, we make the assumption that the polarization varies linearly along the transfer tube and then dropping common factors gives:

$$d_{\text{tc}} f_{\text{tc}} L_{\text{tt}} = d_{\text{tc}}^{\text{tt}} f_{\text{tc}} x L_{\text{tt}} = d_{\text{pc}}^{\text{tt}} f_{\text{pc}} \left(1 - x\right) L_{\text{tt}} \tag{114}$$

where x is the "fractional distance" along the physical transfer tube length where the virtual chamber "is located." To recap, assuming a constant nuclei flux, a linear temperature gradient along the transfer tube, and a linear polarization gradient along the transfer tube, we get the following relationship among the diffusion rates for the two chamber and three chamber systems:

$$f_{\text{tc}}\left(\frac{1}{f_{\text{tc}} d_{\text{tc}}^{\text{tt}}} + \frac{1}{f_{\text{pc}} d_{\text{pc}}^{\text{tt}}}\right) = f_{\text{tc}}\left(\frac{x}{d_{\text{tc}} f_{\text{tc}}} + \frac{1 - x}{d_{\text{tc}} f_{\text{tc}}}\right) = \frac{1}{d_{\text{tc}}} \tag{115}$$

23

over solid	Li	Na	K	Rb	Cs
A'_{vp}	5.667	5.298	4.961	4.857	4.711
B'_{vp}	8310 K	5603 K	4646 K	4215 K	3999 K
A_{vp}	24.57	23.73	22.95	22.71	22.37
B_{vp}	19134 K	12901 K	10698 K	9705 K	9208 K
melting point, K	453.7	370.87	336.53	312.46	301.59
melting point, °C	180.5	97.72	63.38	39.31	28.44
over liquid	**Li**	**Na**	**K**	**Rb**	**Cs**
A'_{vp}	5.055	4.704	4.402	4.312	4.165
B'_{vp}	8023 K	5377 K	4453 K	4040 K	3830 K
A_{vp}	23.17	22.36	21.66	21.45	21.12
B_{vp}	18474 K	12381 K	10253 K	9302 K	8819 K

Table 9: Vapor Pressure Constants for the Alkali Metals. Data from 1995 CRC [41]. Vapor pressure in atm is given as: v.p. $= 10^{A'_{vp} - B'_{vp}/T} = \left(\frac{1 \text{ atm}}{101325 \text{ Pa}} \right) \exp \left(A_{vp} - B_{vp}/T \right)$

which insures that the three chamber solutions Eqs. (111) & (112) reduce to the two chamber solutions Eqs. (17) & (18) in the limit that the fraction of nuclei in the transfer tube approaches zero.

The most significant source of spin relaxation in the transfer tube is spin exchange with alkali vapor. This vapor has a negligible polarization since it is not directly exposed to laser light. Because there is a temperature gradient along the transfer tube, there is also an alkali vapor density gradient as well as ^{3}He density gradient. Therefore we collapse the alkali density gradient into a ^{3}He density weighted average alkali density:

$$\langle [A] \rangle_{tt} = \frac{\int_0^{L_{tt}} [A](z) n(z) \; dz}{\int_0^{L_{tt}} n(z) \; dz} = \frac{\int_{T_{pc}}^{T_{tc}} [A](T) \left(\frac{P}{RT} \right) \left(\frac{L \; dT}{T_{tc} - T_{pc}} \right)}{\int_{T_{pc}}^{T_{tc}} \left(\frac{P}{RT} \right) \left(\frac{L \; dT}{T_{tc} - T_{pc}} \right)} = \frac{\int_{T_{pc}}^{T_{tc}} [A](T) \frac{dT}{T}}{\int_{T_{pc}}^{T_{tc}} \frac{dT}{T}} \tag{116}$$

The temperature dependence of the alkali density is obtained from the the vapor pressure curve combined with the ideal gas law:

$$[A](T) = \frac{\exp \left(A_{vp} - \frac{B_{vp}}{T} \right)}{RT} = \exp \left[-B_{vp} \left(T^{-1} - T_{pc}^{-1} \right) \right] \left(\frac{T_{pc}}{T} \right) [A]_{pc} \tag{117}$$

where A_{pc} & B_{pc} are the vapor pressure constants listed in Tab. (9) and $[A]_{pc}$ is the alkali density in the pumping chamber. Plugging in this form of the alkali density and performing the intergral in the numerator:

$$
\begin{aligned}
\int_{T_{pc}}^{T_{tc}} [A](T) \frac{dT}{T} &= T_{pc} [A]_{pc} \exp \left(\frac{B_{vp}}{T_{pc}} \right) \int_{T_{pc}}^{T_{tc}} \frac{\exp \left(-\frac{B_{vp}}{T} \right)}{T^2} \; dT \\
&= \frac{T_{pc}}{B_{vp}} [A]_{pc} \exp \left(\frac{B_{vp}}{T_{pc}} \right) \left[\exp \left(-\frac{B_{vp}}{T_{tc}} \right) - \exp \left(-\frac{B_{vp}}{T_{pc}} \right) \right] \\
&= \frac{T_{pc}}{B_{vp}} [A]_{pc} \left[-1 + \exp \left(\frac{B_{vp}}{T_{pc}} - \frac{B_{vp}}{T_{tc}} \right) \right] \\
&= \frac{T_{tc} [A]_{tc} - T_{pc} [A]_{pc}}{B_{vp}}
\end{aligned}
\tag{118}
$$

Dividing this by the integral in the denominator gives:

$$\langle [A] \rangle_{tt} = \frac{T_{pc} [A]_{pc} - T_{tc} [A]_{tc}}{B_{vp} \log \left(\frac{T_{pc}}{T_{tc}} \right)} \tag{119}$$

T	[Rb]	$1/\gamma_{se}$	[K]	$1/\gamma_{se}$	[Na]	$1/\gamma_{se}$
(°C)	(10^{14} cm^{-3})	(hrs)	(10^{14} cm^{-3})	(hrs)	(10^{14} cm^{-3})	(hrs)
25.0	1.29×10^{-4}	3.17×10^5	5.88×10^{-6}	7.74×10^6	7.88×10^{-9}	5.78×10^9
50.0	1.47×10^{-3}	2.79×10^4	8.71×10^{-5}	5.23×10^5	2.07×10^{-7}	2.20×10^8
75.0	1.08×10^{-2}	3.80×10^3	8.62×10^{-4}	5.28×10^4	3.37×10^{-6}	1.35×10^7
100.0	6.01×10^{-2}	680	5.78×10^{-3}	7.87×10^3	3.87×10^{-5}	1.18×10^6
125.0	0.270	152	3.04×10^{-2}	1.50×10^3	2.91×10^{-4}	1.56×10^5
150.0	1.01	40.6	0.131	347	1.72×10^{-3}	2.64×10^4
175.0	3.25	12.6	0.478	95.2	8.32×10^{-3}	5.47×10^3
180.4	4.09	10.0	0.621	73.4	1.14×10^{-2}	3.99×10^3
200.0	9.21	4.40	1.52	30.0	3.39×10^{-2}	1.34×10^3
225.0	23.5	1.74	4.28	10.6	0.120	380
226.6	24.8	1.65	4.55	10.0	0.129	352
241.2	40.9	1.00	7.92	5.75	0.254	179
250.0	54.5	0.750	10.9	4.18	0.374	122
275.0	117	0.349	25.4	1.79	1.05	43.4
293.7	198	0.206	45.5	1.00	2.14	21.3
300.0	235	0.174	55.0	0.829	2.69	16.9
315.0	346	0.118	84.5	0.539	4.55	10.0
325.0	443	9.23×10^{-2}	111	0.409	6.36	7.16
350.0	794	5.15×10^{-2}	212	0.214	14.0	3.25
375.0	1.36×10^3	3.01×10^{-2}	385	0.118	29.0	1.57
391.6	1.89×10^3	2.16×10^{-2}	557	8.17×10^{-2}	45.5	1.00
400.0	2.23×10^3	1.84×10^{-2}	667	6.82×10^{-2}	56.7	0.803

Table 10: Pure Alkali Number Density and ^{3}He Spin-Exchange Rate vs. Temperature.

The average alkali spin-exchange rate in the transfer tube is:

$$\langle\gamma_{se}\rangle_{tt} = \gamma_{se}\left(\frac{T_{pc}}{B_{vp}\log\left(\frac{T_{pc}}{T_{tc}}\right)}\right) \tag{120}$$

where we've taken advantage of the fact that, under typical operating conditions, the alkali density in the target chamber is negligible, see Tab. (10).

In principle, the same type of calculation should be done for all other sources of spin relaxation in the transfer tube, such as the nuclear dipolar relaxation. However, since:

1. the spin exchange with essentially unpolarized alkali vapor dominates the spin relaxation

2. the nuclear dipolar relaxation has a soft temperature dependence

3. we ignore, if any, the temperature dependence of the wall relaxation

it is much easier to simply use the geometric mean of the pumping chamber relaxation rate and the total non-beam related relaxation for the target chamber, which gives:

$$\Gamma_{tt} = \langle\gamma_{se}\rangle_{tt} + \langle\Gamma_{dip}\rangle_{tt} + \langle\Gamma_{wall}\rangle_{tt} + \langle\Gamma_{other}\rangle_{tt} \approx \langle\gamma_{se}\rangle_{tt} + \sqrt{\Gamma_{pc}\Gamma_{tc}^0} \tag{121}$$

3.3 Polarization Gradient Between the Pumping and Target Chambers

The polarization gradient between the two chambers is given by:

$$\Delta \equiv 1 - \frac{P_{\text{tc}}^\infty}{P_{\text{pc}}^\infty} = 1 - \left[1 + \Gamma_{\text{tc}}f_{\text{tc}}\left(\frac{1}{f_{\text{tc}}d_{\text{tc}}^{\text{tt}}} + \frac{1}{f_{\text{pc}}d_{\text{pc}}^{\text{tt}}}\right) + \left(1 + \frac{\Gamma_{\text{tc}}}{d_{\text{tc}}^{\text{tt}}}\right)\left(\frac{f_{\text{tt}}}{f_{\text{pc}}}\right)\left(\frac{\Gamma_{\text{tt}}}{d_{\text{pc}}^{\text{tt}}}\right)\right]^{-1} \tag{122}$$

Assuming a linear polarization gradient along the physical transfer tube and placing the third virtual chamber half way between the two chambers gives the following:

$$2d_{\text{tc}}f_{\text{tc}} = d_{\text{tc}}^{\text{tt}}f_{\text{tc}} = d_{\text{pc}}^{\text{tt}}f_{\text{pc}} \tag{123}$$

Note that this amounts to choosing $x = 1/2$ in Eq. (114). Using the above relationship and Eq. (115) allows us to write the polarization gradient as:

$$\Delta_{3\text{ chamber}} = 1 - \left[1 + \frac{\Gamma_{\text{tc}}}{d_{\text{tc}}} + \left(1 + \frac{\Gamma_{\text{tc}}}{2d_{\text{tc}}}\right)\left(\frac{f_{\text{tt}}}{f_{\text{tc}}}\right)\left(\frac{\Gamma_{\text{tt}}}{2d_{\text{tc}}}\right)\right]^{-1} \tag{124}$$

which should be compared to the equation for a two chamber cell neglecting the transfer tube volume:

$$\Delta_{2\text{ chamber}} = 1 - \left[1 + \frac{\Gamma_{\text{tc}}}{d_{\text{tc}}}\right]^{-1} \tag{125}$$

We will now perform a binomial expansion to estimate the size of (1) the polarization loss in the transfer tube and (2) the lowest order term of the polarization gradient. Under typical conditions, the diffusion rate d_{tc} is faster than the relaxation rates in the transfer and target chamber. Applying this approximation to second order in d_{tc} gives:

$$\Delta = 1 - \left(1 - \left[\Gamma_{\text{tc}} + \frac{\Gamma_{\text{tt}}}{2}\frac{f_{\text{tt}}}{f_{\text{tc}}}\right]d_{\text{tc}}^{-1} + \left[\Gamma_{\text{tc}}^2 + \frac{\Gamma_{\text{tt}}^2}{4}\frac{f_{\text{tt}}^2}{f_{\text{tc}}^2} + \frac{3\Gamma_{\text{tc}}\Gamma_{\text{tt}}}{4}\frac{f_{\text{tt}}}{f_{\text{tc}}}\right]d_{\text{tc}}^{-2}\right) + \mathcal{O}\left(\frac{\Gamma_{\text{tc}}^3}{d_{\text{tc}}^3}\right) \tag{126}$$

$$= \left[1 + \frac{1}{2}\frac{f_{\text{tt}}}{f_{\text{tc}}}\frac{\Gamma_{\text{tt}}}{\Gamma_{\text{tc}}}\left(1 \underbrace{- \frac{1}{2}\frac{f_{\text{tt}}}{f_{\text{tc}}}\frac{\Gamma_{\text{tt}}}{d_{\text{tc}}} - \frac{3}{2}\frac{\Gamma_{\text{tc}}}{d_{\text{tc}}}}\right) - \frac{\Gamma_{\text{tc}}}{d_{\text{tc}}}\right]\frac{\Gamma_{\text{tc}}}{d_{\text{tc}}} \tag{127}$$

Note that under typical conditions, $f_{\text{tt}}/f_{\text{tc}}$ is roughly the same order of magnitude as $\Gamma_{\text{tc}}/d_{\text{tc}}$. Therefore we can drop the underbraced terms, which are essentially third order, to give the lowest order terms of the polarization gradient:

$$\Delta = \left[1 + \frac{1}{2}\frac{f_{\text{tt}}}{f_{\text{tc}}}\frac{\Gamma_{\text{tt}}}{\Gamma_{\text{tc}}} - \frac{\Gamma_{\text{tc}}}{d_{\text{tc}}}\right]\frac{\Gamma_{\text{tc}}}{d_{\text{tc}}} + \mathcal{O}\left(\frac{\Gamma_{\text{tc}}^3}{d_{\text{tc}}^3}\right) \tag{128}$$

Therefore the polarization lost traversing through the transfer tube is a second order correction. When there is no beam depolarization in the target chamber, the polarization gradient is written as:

$$\Delta_0 = \left[1 + \frac{1}{2}\frac{f_{\text{tt}}}{f_{\text{tc}}}\frac{\Gamma_{\text{tt}}}{\Gamma_{\text{tc}}} - \frac{\Gamma_{\text{tc}}^0}{d_{\text{tc}}}\right]\frac{\Gamma_{\text{tc}}^0}{d_{\text{tc}}} = \left[1 + \frac{1}{2}\left(\frac{\langle\gamma_{\text{se}}\rangle_{\text{tt}}}{\Gamma_{\text{tc}}^0} + \sqrt{\frac{\Gamma_{\text{pc}}}{\Gamma_{\text{tc}}^0}}\right)\frac{f_{\text{tt}}}{f_{\text{tc}}} - \frac{\Gamma_{\text{tc}}^0}{d_{\text{tc}}}\right]\frac{\Gamma_{\text{tc}}^0}{d_{\text{tc}}} \tag{129}$$

where we have used Eq. (121). The relaxation in the target chamber that is independent of the beam current, Γ_{tc}^0, can be estimated from the lifetime of the cell assuming that the wall relaxation is independent of temperature:

$$\Gamma_{\text{lifetime}} = \tau_{\text{lifetime}}^{-1} = \Gamma_{\text{wall}} + \Gamma_{\text{dip}}\left(T_{\text{lifetime}}\right) \tag{130}$$

$$\Gamma_{\text{tc}}^0 = \Gamma_{\text{wall}} + \Gamma_{\text{dip}}\left(T_{\text{tc}}\right) \tag{131}$$

$$= \Gamma_{\text{lifetime}} - \Gamma_{\text{dip}}\left(T_{\text{lifetime}}\right) + \Gamma_{\text{dip}}\left(T_{\text{tc}}\right) \tag{132}$$

$$= \Gamma_{\text{lifetime}}\left[1 + \frac{\Gamma_{\text{dip}}\left(T_{\text{tc}}\right) - \Gamma_{\text{dip}}\left(T_{\text{lifetime}}\right)}{\Gamma_{\text{lifetime}}}\right] \tag{133}$$

where T_{tc} is the target chamber temperature under operating conditions and T_{lifetime} is the target chamber temperature during the lifetime measurement. Note that the target chamber temperature affects both the density of the target chamber and the nuclear dipolar rate constant. Finally, we can write the contributions to the polarization gradient from both sources up to next to leading order:

$$\Delta = \Delta_0 + \Delta_{\text{beam}} \tag{134}$$

$$\Delta_0 = \frac{\Gamma_{\text{tc}}^0}{d_{\text{tc}}} \left[1 + \frac{1}{2} \left(\frac{\langle \gamma_{\text{se}} \rangle_{\text{tt}}}{\Gamma_{\text{tc}}^0} + \sqrt{\frac{\Gamma_{\text{pc}}}{\Gamma_{\text{tc}}^0}} \right) \frac{f_{\text{tt}}}{f_{\text{tc}}} - \frac{\Gamma_{\text{tc}}^0}{d_{\text{tc}}} \right] \tag{135}$$

$$\Delta_{\text{beam}} = \frac{\Gamma_{\text{beam}}}{d_{\text{tc}}} \left[1 - \frac{\left(2\Gamma_{\text{tc}}^0 + \Gamma_{\text{beam}} \right)}{d_{\text{tc}}} \right] \tag{136}$$

It is now useful to enumerate every assumption and approximation used to derive these relationships:

1. The transfer tube volume is very small compared to the volume of the cell.

2. The target chamber has a negligible vapor pressure of alkali metal.

3. The alkali vapor reaches equilbrium polarization very fast relative to the ^{3}He polarization.

4. The alkali polarization is independent of the ^{3}He polarization.

5. The cell is at thermal equilbrium throughout the ^{3}He polarization process.

6. The diffusion rates per nucleus are the fastest rates in the system.

7. The beam energy is in the range of 1–16 GeV.

8. Only a tiny fraction of the ^{3}He atoms in the target chamber are ionized at any instant of time.

9. Very little of the ionization is due to bremsstrahlung.

10. The electrons created during ionization contribute little to the beam depolarization.

11. Diffusion in the radial direction of the target chamber is essentially instantaneous.

12. Molecular ^{3}He ions contribute little to the beam depolarization.

13. There is a linear temperature gradient along the transfer tube.

14. There is a constant polarization flux through the transfer tube.

15. The wall relaxation is uniform throughout the cell and independent of temperature.

3.4   Discussion and Representative Examples

To get a qualitative and lowest order quantitative handle on the polarization gradient, we'll drop all the higher order terms (including the polarization lost in the transfer tube). Using the reasonable approximation that $\Gamma_{\text{tc}}^0 = \Gamma_{\text{lifetime}}$, the beam independent polarization gradient becomes:

$$\Delta_0 = \frac{\Gamma_{\text{tc}}^0}{d_{\text{tc}}} + \text{higher order terms} \tag{137}$$

$$= \left(\frac{1 \text{ hr}}{6488.21 \text{ cm}^2 \cdot \text{amg}} \right) \left(\frac{L_{\text{tt}} \cdot V_{\text{tc}} \cdot n_{\text{tc}}}{\tau_{\text{lifetime}} \cdot A_{\text{tt}} \cdot \Upsilon \left(T_{\text{pc}}, T_{\text{tc}} \right)} \right) \tag{138}$$

$$= \left(\frac{1}{36} \right) \left(\frac{40 \text{ hrs}}{\tau_{\text{lifetime}}} \right) \left(\frac{0.5 \text{ cm}^2}{A_{\text{tt}}} \right) \left(\frac{L_{\text{tt}}}{6 \text{ cm}} \right) \left(\frac{V_{\text{tc}}}{80 \text{ cm}^3} \right) \left(\frac{n_{\text{tc}}}{10 \text{ amg}} \right) \left(\frac{4/3}{\Upsilon \left(T_{\text{pc}}, T_{\text{tc}} \right)} \right) \tag{139}$$

and the beam dependent polarization gradient is:

$$\Delta_{\text{beam}} = \frac{\Gamma_{\text{ion}} n_a}{d_{\text{tc}}} + \text{higher order terms} \tag{140}$$

$$= \left(\frac{1}{648821 \ \mu\text{A} \cdot \text{amg}}\right) \left(\frac{I \cdot n_a \cdot L_{\text{tc}} \cdot L_{\text{tt}} \cdot n_{\text{tc}}}{A_{\text{tt}} \cdot \Upsilon\left(T_{\text{pc}}, T_{\text{tc}}\right)}\right) \tag{141}$$

$$= \left(\frac{1}{36}\right) \left(\frac{I}{10 \ \mu\text{A}}\right) \left(\frac{n_a}{0.5}\right) \left(\frac{L_{\text{tc}}}{40 \ \text{cm}}\right) \left(\frac{0.5 \ \text{cm}^2}{A_{\text{tt}}}\right) \left(\frac{L_{\text{tt}}}{6 \ \text{cm}}\right) \left(\frac{n_{\text{tc}}}{10 \ \text{amg}}\right) \left(\frac{4/3}{\Upsilon\left(T_{\text{pc}}, T_{\text{tc}}\right)}\right) \tag{142}$$

Both sources contribute equals amounts to the polarization gradient ($\Delta_0 = \Delta_{\text{beam}}$) to lowest order when the following relationship between cell lifetime and beam current is true:

$$I \cdot \tau_{\text{lifetime}} = \left(400 \ \mu\text{A} \cdot \text{hrs} \cdot \text{cm}^2\right) \left(\frac{A_{\text{tc}}}{2.0 \ \text{cm}^2}\right) \left(\frac{0.5}{n_a}\right) \tag{143}$$

In other words, the contribution to the total polarization gradient due to a beam current of 10 μA in a cell with a lifetime of 40 hrs is the same. Some representative values for past experiments are given in Tab. (11) assuming a beam current of 10 μA and a cell lifetime of 40 hr. The lowest order, next to leading order, and full calculation for both a 2 chamber and 3 chamber cell model all produce that same polarization gradient within 10 percent relative. The parameter that varies largest on a cell to cell basis is the transfer tube cross sectional area. Unfortunately the polarization gradient also happens to be very sensitive to this parameter. Increasing the relative amount of N_2 in the cell helps suppress beam depolarization. Alternatively, a long lifetime cell helps suppress the polarization gradient that is indepedent of the beam. The largest uncertainty comes from our imprecise knowledge of the various ionic rate constants used to calculate the beam depolarization. In practical terms, n_a is known to only about 15 percent.

The next largest souce of uncertainty is in our knowledge of the wall relaxation. The target chamber has a larger surface area to volume ratio than the pumping chamber, so, naively, one would imagine that the wall relaxation would be greater in the target chamber. We also don't know its temperature dependence; however, the relative change in the target chamber temperature is at the level of 10 percent. Finally, we use a fairly simple diffusion model to estimate the diffusion rates per nucleus. If we apply a 10 percent uncertainty to the diffusion rates as well, then our overall uncertainty is about 20 percent relative on a usually 5 percernt relative correction.

3.5 Estimating Diffusion and Beam Parameters Empirically

In principle, it is possible to estimate these parameters empirically from data rather than having to rely upon theoretical calculations. To obtain information on the diffusion rates, spin-up data can be taken on the target chamber, or even better both chambers, and then fit to Eq. (15). This method would probably benefit from taking spin-up data under different initial conditions, for example:

1. Start with both chambers at zero polarization, $P_{\text{tc}}^0 = 0$ and $P^0\text{pc} = 0$.

2. Start with both chambers at the opposite polarization, $P_{\text{tc}}^0 = -P_{\text{tc}}^\infty$ and $P_{\text{pc}}^0 = -P_{\text{pc}}^\infty$. This could easily be accomplished by reversing the spins by AFP after the polarization has reached equilibrium.

3. Start with one chamber at the equilibrium polarization, while the other chamber is at zero, $P_{\text{tc}}^0 = 0$ and $P_{\text{pc}}^0 = +P_{\text{pc}}^\infty$. This could be accomplished by a transient burst of on-resonance RF localized near the target chamber.

To obtain information about the beam depolarization, one can compare the equilibrium polarizations with beam on and off. This works best when the diffusions rates are much faster than all other rates. Under those conditions:

$$P^\infty = P_{\text{pc}}^\infty = P_{\text{tc}}^\infty = \frac{P_A \gamma_{\text{se}} f_{\text{pc}}}{\gamma_{\text{se}} f_{\text{pc}} + \Gamma_{\text{pc}} f_{\text{pc}} + \Gamma_{\text{tc}} f_{\text{tc}}} \tag{144}$$

$$P_{\text{off}}^\infty = \frac{P_A \gamma_{\text{se}} f_{\text{pc}}}{\gamma_{\text{se}} f_{\text{pc}} + \Gamma_{\text{pc}} f_{\text{pc}} + \Gamma_{\text{tc}}^0 f_{\text{tc}}} \tag{145}$$

parameter	E154	GDH	A1n	g2n	saGDH	GEn-spc	GEn-LPC	units
$[^3\mathrm{He}]_{\mathrm{fill}}$	8.83	9.62	8.69	8.19	8.78	8.25	7.40	amg
$[\mathrm{N}_2]_{\mathrm{fill}}$	0.0776	0.0964	0.0824	0.0940	0.0913	0.125	0.112	amg
R_{pc}	2.62	2.94	3.02	3.02	2.93	2.90	4.12	cm
A_{tt}	0.709	1.01	0.537	0.537	0.645	0.385	0.385	cm^2
L_{tt}	6.2	6.02	6.52	6.52	6.11	10.1	8.89	cm
A_{tc}	3.56	2.27	2.05	2.05	2.47	2.03	2.03	cm^2
L_{tc}	29.8	39.6	25.6	39.5	39.5	40.3	40.3	cm
T_{pc}	465	492	505	505	485	558	558	K
T_{tc}	343	330	333	333	331	309	309	K
V_{pc}	75.0	106	115	115	105	102	292	cm^3
V_{tt}	4.39	6.08	3.50	3.50	3.94	3.88	3.42	cm^3
V_{tc}	106	89.8	52.4	80.9	97.5	81.8	81.8	cm^3
t	1.35	1.49	1.51	1.51	1.46	1.80	1.80	-
v	0.71	1.18	2.19	1.42	1.07	1.24	3.58	-
f_{pc}	0.343	0.442	0.591	0.484	0.424	0.408	0.664	-
f_{tt}	0.023	0.030	0.021	0.017	0.019	0.020	0.010	-
f_{tc}	0.656	0.557	0.408	0.515	0.575	0.591	0.335	-
n_{pc}	7.31	7.85	7.48	6.75	7.17	6.07	6.29	amg
n_{tc}	9.90	11.7	11.34	10.23	10.51	10.96	11.36	amg
p_{op}	12.4	14.1	13.8	12.4	12.7	12.4	12.8	atm
ρ	0.87	1.00	0.94	1.14	1.03	1.51	1.51	-
Ω	0.366	0.309	0.319	0.354	0.345	0.33	0.319	rad
r	18.0	15.4	16.0	16.2	16.4	14.0	13.7	-
n_a	0.5191	0.3998	0.4243	0.4761	0.4672	0.4066	0.3849	-
n_m^{max}	0.0012	0.0007	0.0008	0.0008	0.0008	0.0005	0.0004	-
τ_{beam}	68.5	56.7	48.3	43.0	52.8	49.9	52.7	hr
τ_{tc}^0	38.7	36.7	35.7	36.7	37.3	35.1	33.2	hr
τ_{tc}	24.7	22.2	20.5	19.8	21.8	20.6	20.3	hr
τ_{tt}	19.9	11.8	8.3	8.3	13.8	9.4	9.3	hr
Υ	1.3	1.32	1.33	1.33	1.31	1.35	1.35	-
d_{pc}^{-1}	0.566	0.581	1.207	1.089	0.839	1.846	4.828	hr
d_{tc}^{-1}	1.081	0.731	0.832	1.159	1.138	2.669	2.434	hr
Δ_0^0, Eq. (137)	2.79	1.99	2.32	3.15	3.05	7.59	7.32	% rel.
Δ_0^1, Eq. (135)	2.81	2.12	2.54	3.29	3.09	7.51	7.19	% rel.
Δ_{beam}^0, Eqn. (142)	1.57	1.28	1.72	2.69	2.15	5.34	4.61	% rel.
Δ_{beam}^1, Eqn. (136)	1.46	1.22	1.61	2.45	1.97	4.24	3.72	% rel.
Δ^0, Eqn. (137;142)	4.37	3.28	4.05	5.84	5.20	12.9	11.9	% rel.
Δ^1, Eqn. (135;136)	4.27	3.34	4.15	5.74	5.07	11.8	10.9	% rel.
Δ_{2ch}, Eqn. (125)	4.18	3.17	3.89	5.52	4.94	11.4	10.7	% rel.
Δ_{3ch}, Eqn. (124)	4.27	3.34	4.14	5.74	5.07	11.9	11.0	% rel.

Table 11: Polarization Gradient for Representative Cells with $I = 10\ \mu$A and $\tau_{\mathrm{lifetime}} = 40$ hr.

$$P_{\text{on}}^{\infty} = \frac{P_A \gamma_{\text{se}} f_{\text{pc}}}{\gamma_{\text{se}} f_{\text{pc}} + \Gamma_{\text{pc}} f_{\text{pc}} + \Gamma_{\text{tc}}^0 f_{\text{tc}} + \Gamma_{\text{beam}} f_{\text{tc}}} \tag{146}$$

$$\frac{P_{\text{off}}^{\infty}}{P_{\text{on}}^{\infty}} = 1 + \frac{\Gamma_{\text{beam}} f_{\text{tc}}}{\gamma_{\text{se}} f_{\text{pc}} + \Gamma_{\text{pc}} f_{\text{pc}} + \Gamma_{\text{tc}}^0 f_{\text{tc}}} = 1 + \tau_{\text{slow}}^{\text{off}} \Gamma_{\text{beam}} f_{\text{tc}} \tag{147}$$

$$\Gamma_{\text{beam}} = \frac{\Gamma_{\text{s}}^{\text{off}}}{f_{\text{tc}}} \left[\frac{P_{\text{off}}^{\infty}}{P_{\text{on}}^{\infty}} - 1 \right] \tag{148}$$

This method requires knowledge of the "slow" spin-up time constant with the beam off, Γ_{s}.

3.6 Polarization Gradient Within the Target Chamber

Thus far we've assumed that the polarization is uniform throughout the target chamber. However, the polarization at the ends of the target chamber must be lower than the polarization at the junction between the transfer tube and the targer chamber. In addition, the beam depolarizes only within an area defined by the beam raster. To account for a spatial variation in polarization due to these effects, we'll model the transfer tube-target chamber junction as a delta function source for polarization and the beam raster area as a sink for polarization. Therefore, Eq. (8) is generalized to:

$$\frac{dP_{\text{tc}}(r, z, t)}{dt} = d_{\text{tc}} \mathcal{A} \left(P_{\text{pc}} - P_{\text{tc}} \right) \delta(z) \delta(r - r_{\text{tc}}) - \left(\Gamma_{\text{tc}}^0 + \Gamma_{\text{beam}} \Theta(r - r_0) \right) P_{\text{tc}} + D \nabla^2 P_{\text{tc}} \tag{149}$$

where $\mathcal{A}$ is the characteristic area of the polarization source, $\Theta(r - r_0)$ is the Heaviside function, r_0 is the radius of the beam raster, and D is the diffusion constant evaluated at the target chamber temperature and density.

To solve this equation, we'll have to make some simplifying arguments. First, we will consider the system only at equilibrium, $t \to \infty$; therefore the polarization has reached a steady state value throughout the cell, $dP_{\text{tc}}/dt = 0$. Second, we will assume that the polarization dynamics within the pumping chamber are sensitive to only the volume averaged target chamber polarization $\langle P_{\text{tc}} \rangle$ (as opposed to some small region localized near the transfer tube-target chamber junction). This is true when the diffusion rates are fast relative to all other polarization/relaxation rates in the cell. This implies that P_{tc}^{∞} in all previous equations is to be interpreted as the volume averaged target chamber polarization.

Third, we will assume that the gradient in the radial direction is negligible relative to the gradient in the longitudinal direction. To justify this assumption, consider the characteristic distance that a ^{3}He atom travels during the characteristic relaxation time under typical conditions:

$$\lambda = \sqrt{\frac{D}{\Gamma_{\text{tc}}}} \approx \sqrt{\frac{0.2 \text{ cm}^2/\text{sec}}{1/20 \text{ hrs}^{-1}}} \approx 120 \text{ cm} \tag{150}$$

The polarization gradient within the target chamber scales as the ratio between the characteristic size and this characteristic diffusion length:

$$\frac{r_{\text{tc}} = 0.85 \text{ cm}}{\lambda} \approx 0.007 \ll \frac{L_{\text{tc}}/2 = 20 \text{ cm}}{\lambda} \approx 0.17 < 1 \tag{151}$$

This justifies our third assumption and finally we get:

$$0 = d_{\text{tc}} \ell \left(P_{\text{pc}}^{\infty} - \langle P_{\text{tc}} \rangle \right) \delta(z) - \Gamma_{\text{tc}} P_{\text{tc}} + D \frac{d^2 P_{\text{tc}}}{dz^2} \tag{152}$$

where ℓ is the characteristic size of the polarization source. Note the we have tacitly defined the coordinate system such that the transfer tube-target chamber junction occurs at $z = 0$ and the target chamber ends are at $z = \pm L_{\text{tc}}/2$.

Finally we can solve this equations by performing a Laplace transform and solving for $\mathcal{L} P_{\text{tc}}$:

$$-\Gamma_{\text{tc}} \mathcal{L} P_{\text{tc}} + D \left[k_z^2 \mathcal{L} P_{\text{tc}} - k_z P_{\text{tc}}(0) - P_{\text{tc}}'(0) \right] = -d_{\text{tc}} \ell \left(P_{\text{pc}}^{\infty} - \langle P_{\text{tc}} \rangle \right)$$

$$\left[-\Gamma_{\text{tc}} + D k_z^2 \right] \mathcal{L} P_{\text{tc}} = D k_z P_{\text{tc}}(0) + D P_{\text{tc}}'(0) - d_{\text{tc}} \ell \left(P_{\text{pc}}^{\infty} - \langle P_{\text{tc}} \rangle \right)$$

$$\mathcal{L} P_{\text{tc}} = \frac{k_z P_{\text{tc}}(0) + P_{\text{tc}}'(0) - \frac{d_{\text{tc}} \ell}{D} \left(P_{\text{pc}}^{\infty} - \langle P_{\text{tc}} \rangle \right)}{k_z^2 - \frac{\Gamma_{\text{tc}}}{D}} \tag{153}$$

where k_z is the conjugate variable to z and $P_{tc}(0)$ & $P'_{tc}(0)$ are the polarization and first derivative of the polarization evaluated at $z = 0$. Substituting the characterisitic diffusion length and taking the inverse Laplace transform gives:

$$
\begin{aligned}
\mathcal{L}P_{tc} &= \frac{k_z P_{tc}(0) + P'_{tc}(0) - \frac{d_{tc}\ell}{D}\left(P_{pc}^\infty - \langle P_{tc}\rangle\right)}{k_z^2 - \lambda^{-2}} \\
\mathcal{L}^{-1}\mathcal{L}P_{tc} &= P_{tc}(0)\mathcal{L}^{-1}\left(\frac{k_z}{k_z^2 - \lambda^{-2}}\right) + \lambda\left[P'_{tc}(0) - \frac{d_{tc}\ell}{D}\left(P_{pc}^\infty - \langle P_{tc}\rangle\right)\right]\mathcal{L}^{-1}\left(\frac{\lambda^{-1}}{k_z^2 - \lambda^{-2}}\right) \\
P_{tc}(z) &= P_{tc}(0)\cosh\left(\frac{z}{\lambda}\right) + \lambda\left[P'_{tc}(0) - \frac{d_{tc}\ell}{D}\left(P_{pc}^\infty - \langle P_{tc}\rangle\right)\right]\sinh\left|\frac{z}{\lambda}\right|
\end{aligned}
\tag{154}
$$

The inverse Laplace transforms performed above are only valid for $|k_z|\lambda > 1$ or analogously $|z| < \lambda$. Since $\lambda \approx 120$ cm and the maximum value is $|z| = L_{tc}/2 = 20$ cm, the above solution is valid and we can expand the hyperbolic trig functions to lowest order to give:

$$
P_{tc}(z) = P_{tc}(0) + |z|\left[P'_{tc}(0) - \frac{d_{tc}\ell}{D}\left(P_{pc}^\infty - \langle P_{tc}\rangle\right)\right] + \mathcal{O}\left(\frac{|z|}{\lambda}\right)^2
\tag{155}
$$

The value of the first derivative of the polarization at $z = 0$ can be estimated by analogy to Eq. (79):

$$
J_{tc}(z) = n_{tc}DP'_{tc}(z)
\tag{156}
$$

We'll assume that the net total number of particles entering the target chamber at the transfer tube-target chamber junction is conserved, which implies:

$$
J_{tt}A_{tt} = \left[J_{tc}(\text{at 0 towards } +z) + J_{tc}(0\text{at 0 towards } -z)\right]A_{tc}
\tag{157}
$$

Note that the number of particles entering the target chamber are equally split and directed towards either end of the target chamber. Combining this with Eq. (84) gives:

$$
P'_{tc}(0) = \frac{J_{tc}(0)}{n_{tc}D} = \frac{1}{2}\frac{A_{tt}}{A_{tc}}\frac{J_{tt}}{n_{tc}D} = \frac{d_{tc}L_{tc}}{2D}\left(\langle P_{tc}\rangle - P_{pc}^\infty\right)
\tag{158}
$$

The difference in polarization at equilibrium between the two chambers is obtained from Eq. (18):

$$
P_{pc}^\infty - \langle P_{tc}\rangle = \langle P_{tc}\rangle\left(1 + \frac{\Gamma_{tc}}{d_{tc}}\right) - \langle P_{tc}\rangle = \langle P_{tc}\rangle\frac{\Gamma_{tc}}{d_{tc}}
\tag{159}
$$

Putting this altogether, calculating the average value of P_{tc} along the target chamber, and solving for $P_{tc}(0)$:

$$
\begin{aligned}
\langle P_{tc}\rangle = \frac{1}{L_{tc}}\int_{-L_{tc}/2}^{+L_{tc}/2}P_{tc}(z)\,dz &= \frac{1}{L_{tc}}\int_{-L_{tc}/2}^{+L_{tc}/2}P_{tc}(0) - |z|\langle P_{tc}\rangle\frac{\Gamma_{tc}}{D}\left(\ell + \frac{L_{tc}}{2}\right)\,dz
\end{aligned}
\tag{160}
$$

$$
= P_{tc}(0) - \frac{L_{tc}}{4}\langle P_{tc}\rangle\frac{\Gamma_{tc}}{D}\left(\ell + \frac{L_{tc}}{2}\right)\,dz
\tag{161}
$$

$$
P_{tc}(0) = \langle P_{tc}\rangle\left[1 + \frac{L_{tc}}{4}\frac{\Gamma_{tc}}{D}\left(\ell + \frac{L_{tc}}{2}\right)\right]
\tag{162}
$$

Finally, using this form of $P_{tc}(0)$ and rearranging a few things gives:

$$
P_{tc}(z) = \langle P_{tc}\rangle\left[1 + \left(1 - \frac{4|z|}{L_{tc}}\right)\left(1 + \frac{2\ell}{L_{tc}}\right)\left(\frac{L_{tc}^2}{8}\right)\frac{\Gamma_{tc}}{D}\right]
\tag{163}
$$

The total center to end relative polarization gradient is given by:

$$
\frac{\Delta P_{tc}}{\langle P_{tc}\rangle} = \left(1 + \frac{2\ell}{L_{tc}}\right)\left(\frac{L_{tc}^2}{4}\right)\frac{\Gamma_{tc}}{D}
\tag{164}
$$

Finally, to quantify things, we need to estimate ℓ, the characteristic size of the polarization source. In this case, the "polarization source" is the transfer tube; therefore it's reasonable to use the transfer tube diameter or the square root of the transfer tube cross sectional area. For $\ell = \sqrt{A_{\mathrm{tt}}} \ll L_{\mathrm{tc}}$, we find:

$$\frac{\Delta P_{\mathrm{tc}}}{\langle P_{\mathrm{tc}} \rangle} = \left(\frac{1}{36}\right) \left(\frac{L_{\mathrm{tc}}}{40 \text{ cm}}\right)^2 (\Gamma_{\mathrm{tc}} \cdot 20 \text{ hrs}) \left(\frac{n_{\mathrm{tc}}}{10 \text{ amg}}\right) \left(\frac{323.15 \text{ K}}{T_{\mathrm{tc}}}\right)^{0.7} \tag{165}$$

Therefore, under typical conditions, the polarization decreases linearly from the center of the target chamber to the ends. The polarization across the target chamber varies by about ± 2 percent relative to the target chamber average.

References

[1] B. Chann, E. Babcock, L.W. Anderson, and T.G. Walker. Measurements of ^{3}He spin-exchange rates. *Phys. Rev. A*, 66(3):032703, Sep 2002.

[2] Earl Babcock, Ian Nelson, Steve Kadlecek, Bastiaan Driehuys, L.W. Anderson, F.W. Hersman, and Thad G. Walker. Hybrid Spin-Exchange Optical Pumping of He. *Physical Review Letters*, 91(12):123003, 2003.

[3] P.I. Borel, L.V. Sogaard, W.E. Svendsen, and N. Andersen. Spin-exchange and spin-destruction rates for the ^{3}He -Na system. *Physical Review A (Atomic, Molecular, and Optical Physics)*, 67(6):062705, 2003.

[4] N.R. Newbury, A.S. Barton, G.D. Cates, W. Happer, and H. Middleton. Gaseous ^{3}He -^{3}He magnetic dipolar spin relaxation. *Phys. Rev. A*, 48(6):4411–4420, Dec 1993.

[5] M.J. Berger, J.S. Coursey, M.A. Zucker, and J. Chang. *ESTAR, PSTAR, and ASTAR: Computer Programs for Calculating Stopping-Power and Range Tables for Electrons, Protons, and Helium Ions.* (version 1.2.3). [Online] Available: http://physics.nist.gov/Star [2006, November 2]. National Institute of Standards and Technology, Gaithersburg, MD, 2005.

[6] M.J. Berger, J.H. Hubbell, S.M. Seltzer, J. Chang, J.S. Coursey, R. Sukumar, and D.S. Zucker. *XCOM: Photon Cross Section Database.* (version 1.3). [Online] Available: http://physics.nist.gov/xcom [2006, November 2]. National Institute of Standards and Technology, Gaithersburg, MD, 2005.

[7] William R. Leo. *Techniques for Nuclear and Particle Physics Experiments: A How-to Approach.* Springer-Verlag, Berlin, second revised edition, 1994.

[8] R.M. Sternheimer, M.J. Berger, and S.M. Seltzer. Density Effect for the Ionization Loss of Charged Particles In Various Substances. *Atomic Data and Nuclear Data Tables*, 30(2):261–271, March 1984.

[9] H. Bethe and W. Heitler. On the Stopping of Fast Particles and on the Creation of Positive Electrons. *Proceedings of the Royal Society of London. Series A, Containing Papers of a Mathematical and Physical Character*, 146(856):83–112, August 1934.

[10] William P. Jesse and John Sadauskis. Alpha-Particle Ionization in Mixtures of the Noble Gases. *Phys. Rev.*, 88(2):417–418, Oct 1952.

[11] William P. Jesse and John Sadauskis. Alpha-Particle Ionization in Pure Gases and the Average Energy to Make an Ion Pair. *Phys. Rev.*, 90(6):1120–1121, Jun 1953.

[12] T.E. Bortner and G.S. Hurst. Ionization of Pure Gases and Mixtures of Gases by 5-Mev Alpha Particles. *Phys. Rev.*, 93(6):1236–1241, Mar 1954.

[13] G.A. Erskine. The Effect of Contaminating Gases on the Energy per Ion Pair in Helium. *Proceedings of the Physical Society. Section A*, 67(7):640–642, 1954.

[14] R.W. Gurney. Ionisation by Alpha-Particles in Monoatomic and Diatomic Gases. *Proceedings of the Royal Society of London. Series A, Containing Papers of a Mathematical and Physical Character*, 107(742):332–340, February 1925.

[15] J.F. Lehmann. The Absorption of Slow Cathode Rays in Various Gases. *Proceedings of the Royal Society of London. Series A, Containing Papers of a Mathematical and Physical Character*, 115(772):624–639, August 1927.

[16] Hans H. Staub. Detection Methods. In E. Segrè, editor, *Experimental Nuclear Physics, Volume I*, pages 1–165, New York, 1953. John Wiley and Sons.

[17] Bruno Rossi. *High-Energy Physics*. Prentice-Hall, Incorporated, New York, 1952.

[18] L.H. Gray. *Proceedings of the Cambridge Philosophical Society*, 40:72, 1944.

[19] C.J. Bakker and E. Segrè. Stopping Power and Energy Loss for Ion Pair Production for 340-Mev Protons. *Phys. Rev.*, 81(4):489–492, Feb 1951.

[20] Lloyd O. Herwig and Glenn H. Miller. Alpha-Particle Ionization Yields in a Gridded Chamber. *Phys. Rev.*, 94(5):1183, Jun 1954.

[21] W. Haberli, P. Huber, and E. Baldinger. *Helv. Phys. Acta*, 25:467, 1952.

[22] J.M. Valentine. Energy per Ion Pair for Electrons in Gases and Gas Mixtures. *Proceedings of the Royal Society of London. Series A, Mathematical and Physical Sciences*, 211(1104):75–85, February 1952.

[23] Robert H. Frost and Carl E. Nielsen. The Specific Probable Ionization of Electrons Observed with a Wilson Cloud Chamber. *Phys. Rev.*, 91(4):864–870, Aug 1953.

[24] Leon M. Dorfman. Absorption of Tritium Beta Particles in Hydrogen and Other Gases. *Phys. Rev.*, 95(2):393–396, Jul 1954.

[25] William P. Jesse and John Sadauskis. Ionization in Pure Gases and the Average Energy to Make an Ion Pair for Alpha and Beta Particles. *Phys. Rev.*, 97(6):1668–1670, Mar 1955.

[26] Jerome Weiss and William Bernstein. Energy Required to Produce One Ion Pair in Several Noble Gases. *Phys. Rev.*, 103(5):1253, Sep 1956.

[27] W.G. Stone and L.W. Cochran. Ionization of Gases by Recoil Atoms. *Phys. Rev.*, 107(3):702–704, Aug 1957.

[28] Emilio Segrè. *Nuclei and Particles: An Introduction to Nuclear and Subnuclear Physics*. W.A. Benjamin, INC., New York, 1964.

[29] J.M. Valentine and S.C. Curran. Average energy expenditure per ion pair in gases and gas mixtures. *Reports on Progress in Physics*, 21(1):1–29, 1958.

[30] K.D. Bonin, D.P. Saltzberg, and W. Happer. Relaxation of gaseous spin-polarized ^{3}He targets due to creation of ^{3}He$^+$. *Phys. Rev. A*, 38(9):4481–4487, Nov 1988.

[31] K.D. Bonin, T.G. Walker, and W. Happer. Relaxation of gaseous spin-polarized ^{3}He targets due to ionizing radiation. *Phys. Rev. A*, 37(9):3270–3282, May 1988.

[32] Donald Rapp and W.E. Francis. Charge Exchange between Gaseous Ions and Atoms. *The Journal of Chemical Physics*, 37(11):2361–2645, Dec 1962.

[33] J. Heimerl, R. Johnsen, and Manfred A. Biondi. Ion-Molecule Reactions, He$^+$ + O$_2$ and He$^+$ + N$_2$, at Thermal Energies and Above. *The Journal of Chemical Physics*, 51(11):5041–5048, Dec 1969.

[34] J.D.C. Jones, D.G. Lister, D.P. Wareing, and N.D. Twiddy. The temperature dependence of the three-body reaction rate coefficient for some rare-gas atomic ion-atom reactions in the range 100-300 K. *J. Phys. B: Atom. Molec. Phys.*, 13:3247–3255, 1980.

[35] D.K. Bohme, N.G. Adams, M. Mosesman, D.B. Dunkin, and E.E. Ferguson. Flowing Afterglow Studies of the Reactions of the Rare-Gas Molecular Ions He_2^+, Ne_2^+, and Ar_2^+ with Molecules and Rare-Gas Atoms. *The Journal of Chemical Physics*, 52(10):5094–5101, May 1970.

[36] J.M. Pouvesle, A. Bouchoule, and J. Stevefelt. Modeling of the charge transfer afterglow excited by intense electrical discharges in high pressure helium nitrogen mixtures. *The Journal of Chemical Physics*, 77(2):817–825, Jul 1982.

[37] C.B. Collins and F.W. Lee. Measurement of the rate coefficients for the bimolecular and termolecular ion-molecule reactions of He_2^+ with selected atomic and molecular species. *The Journal of Chemical Physics*, 68(4):1391–1401, Feb 1978.

[38] L.D. Landau and E.M. Lifshitz. *Fluid Mechanics (Course of Theoretical Physics, Vol. 6)*. Butterworth-Heinemann, Oxford, second revised engish edition, 1998.

[39] Mikhail V. Romalis. *Laser Polarizaed ^{3}He Target Used for a Precision Measurement of the Neutron Spin Structure*. PhD thesis, Princeton University, 1997.

[40] Xiaochao Zheng. *Precision Measurement of Neutron Spin Asymmetry A_1^n at Large x_{bj} Using CEBAF at 5.7 GeV*. PhD thesis, Massachusetts Institute of Technology, 2002.

[41] David R. Lide (Editor-in Chief). *CRC Handbook of Chemistry and Physics*. CRC Press, Boca Raton, FL, 75th student edition, 1994.